

**Development of magnetic stress detection methods involving a cobalt ferrite composite
stress sensing material and a magnetic imaging system**

by

Jason Allen Paulsen

A thesis submitted to the graduate faculty
in partial fulfillment of the requirements for the degree of
MASTER OF SCIENCE

Major: Mechanical Engineering

Program of Study Committee:
David C. Jiles, Co-major Professor
Palaniappa A. Molian, Co-major Professor
Greg R. Luecke

Iowa State University

Ames, Iowa

2004

Graduate College
Iowa State University

This is to certify that the master's thesis of

Jason Allen Paulsen

has met the thesis requirements of Iowa State University

Signatures have been redacted for privacy

To

Larry & Jan Paulsen

for their support

TABLE OF CONTENTS

| | |
|--|--------|
| CHAPTER 1. INTRODUCTION | 1 |
| Introduction | 1 |
| Magnetic Imaging System | 4 |
| Magnetomechanical Stress Sensing material | 5 |
| Thesis Organization | 6 |
| References | 7 |
| CHAPTER 2. STUDY OF CURIE TEMPERATURE OF COBALT FERRITE BASED COMPOSITES FOR STRESS SENSOR APPLICATIONS | 8 |
| Abstract | 8 |
| Introduction | 9 |
| Materials | 10 |
| Varying Compositions | 10 |
| Varying Sintering Temperatures | 11 |
| Experimental | 12 |
| Results and Discussion | 12 |
| Varying Compositions | 12 |
| Varying Sintering Temperatures | 15 |
| Conclusions | 17 |
| Acknowledgement | 18 |
| References | 18 |
| CHAPTER 3. NEW MANGANESE-SUBSTITUTED COBALT FERRITE MAGNETOSTRICTIVE MATERIALS FOR MAGNETIC STRESS SENSOR APPLICATIONS | 19 |

| | |
|------------------------|----|
| Abstract | 19 |
| Introduction | 20 |
| Experimental Procedure | 21 |
| Results and Discussion | 23 |
| Conclusions | 27 |
| Acknowledgement | 28 |
| References Cited | 28 |

| | |
|--|----|
| CHAPTER 4. DEVELOPMENT OF A MAGNETIC NON- DESTRUCTIVE EVALUATION IMAGING SYSTEM USING MAGNETORESISTIVE DEVICES | 29 |
| Abstract | 29 |
| Introduction | 30 |
| Magnetic Imaging System | 32 |
| Experimental Studies Using the Magnetic Scanning System | 37 |
| Detection of Surface Notches | 37 |
| Detection of Reverse Side Notches | 41 |
| Acknowledgement | 45 |
| References | 45 |

| | |
|--|----|
| CHAPTER 5. QUANTITATIVE EVALUATION OF STRESS DISTRIBUTION IN MAGNETIC MATERIALS BY BARKHAUSEN EFFECT AND MAGNETIC HYSTERESIS MEASUREMENTS | 47 |
| Abstract | 47 |
| Introduction | 48 |
| Experimental Details | 49 |
| Results and Discussion | 52 |

| | |
|--|--------|
| Conclusion | 56 |
| Acknowledgement | 58 |
| References | 58 |
| CHAPTER 6. CONCLUSIONS | 60 |
| Magnetostrictive stress sensing material | 60 |
| Magnetic imaging system | 62 |
| Magnetic stress detection | 63 |

CHAPTER 1. INTRODUCTION

One major problem with the design, operation, and life of many systems involving mechanical, thermal, or electrical components is the presence of stress. Although large amounts of stress can be advantageous in some cases, in most cases it is undesirable and can be detrimental to many materials because it can lead to crack propagation, fatigue damage, and even fracture. In other cases the stresses may be intentional, as for example in the turning moment or torque on a shaft. This does not necessarily cause failure, nevertheless it is desirable to know the stress levels for the purposes of control. Because of this, a cheap and reliable method for detecting and monitoring stress levels in materials is needed. In the past, several different methods have been employed to detect and monitor stress levels, however, with increasing interest in sensor and actuators for automated control, and nondestructive evaluation for monitoring materials degradation, new methods must be developed to more accurately and easily assess the amount of stress in materials.

One type of stress that is usually present in most materials is residual stress. Residual stresses are stresses that persist in a material that is free of external forces or temperature gradients [1]. These residual stresses are usually caused by mechanical or thermal processing of the material and can be induced either intentionally or unintentionally as a result of some processing method. Some residual stresses are intentionally induced, as in the case of shot peening, to increase the resistance to crack propagation. However, most often stresses are created when the material is produced by methods such as forging, rolling, bending, welding, or thermal heat treating. Irrespective of how residual stresses are formed within a material, a

fast, accurate, cheap, and easy way to detect and quantitatively determine the levels of these residual stresses in a material is in great demand.

Currently there are only a few ways to detect the amount of residual stress in a material. These consist of eddy-current measurements, ultrasonic methods, X-ray diffraction, and hole drilling. Most of these methods have some drawbacks because they may be destructive, can be very expensive, are more qualitative than quantitative, or require highly skilled operators. Another drawback to all of the current residual stress measurement methods is that other factors can affect the results from a residual stress measurement. For instance, a small second-phase or sub-surface defect that might be present in a material can show up on the residual stress measurement and be misinterpreted as a local stress concentration.

The other type of stress that can be present in a material is a form of applied or induced stress. This can be caused by some external force acting on a material such as mechanical or thermal sources. Most mechanical, thermal and electrical systems contain some components that are under stress during operation. It may simply be that the level of stress needs to be known, even though it does not constitute a risk of failure (for example for control functions). The application of stress, if above some critical design level, can lead to crack propagation, fatigue damage and even fracture which can be detrimental to many systems. For this reason, the constant monitoring of applied stress levels can be an important feature.

There are quite a few methods for detecting the level of applied stress on materials. Some of these employ the same methods as are used for detecting residual stress along with others which involve measuring the strain of a material and relating that to the applied stress such as with a strain gages, lasers, or optics. Although these methods have been proven and work well, there are some disadvantages in the practical implementation of these methods. Laser and optical methods are quite expensive and require large amount of space and equipment. Electrical resistance strain gages are inexpensive and small, however, they require very accurate instrumentation to determine and condition the small changes in resistance present. The strain gage method is also restricted because the material being tested must be connected to the conditioning instrumentation by wires. This hinders its use in many applications such as measuring the torque on rotating shafts where a non-contact method is essential, or monitoring the point to point differences in the stress levels in different locations in a material or system.

The need for new methods for detecting stress can be found in many industries. One example of the increased demand in stress sensing technology is found with National Aeronautical and Space Administration (NASA). They have recently expressed interest in finding a method for easily and reliably monitoring the amount of stress being applied to the skins and wings of their spacecraft as they enter and leave orbit. Another example of the need for these technologies is in the railroad industry. They are currently looking for a way to quickly monitor the amount of residual stresses present in the rails by scanning a probe over the rails. This would give the rail companies a better idea of when the rails needed to be

replaced to prevent failure. It is shown in this research that the use of magnetic methods can provide a solution to this problem.

The principle of using magnetics to evaluate stress levels has not been as widely investigated as other techniques until recently, however it can be a very useful method. The magnetic properties of a magnetic material can be greatly affected by the presence of a stress through the magnetoelastic coupling. Because of this, the stress state of a material can be determined by simply measuring some of the magnetic properties of the material. A few methods for doing this have been previously investigated and partially employed. One of these methods involves utilizing the magnetomechanical effect. That is the change in magnetization with stress. The other method is by analysis of the stress dependence of the magnetic hysteresis loop and Barkhausen emission noise.

Magnetic imaging system

To utilize the stress dependence of the magnetic hysteresis loop and Barkhausen emission noise, a magnetic imaging system was developed. This system is capable of scanning the surface of a magnetic material and measuring the magnetic properties of the material such as permeability, remanence, coercivity, and hysteresis loss, along with the Barkhausen noise. Figure 1.1 shows an example of how the magnetic hysteresis loop varies with the application of an applied stress. This shows that the loop characteristics such as differential permeability are stress dependent. The stress dependence of these hysteresis properties are measured and the hysteresis properties are then measured on a test material and analyzed to determine the stress. An image can be created to display the stress condition of

the material at different locations across a surface. This system has been proven to be a viable method for detecting surface and sub-surface cracks, thickness variations, along with stress levels.

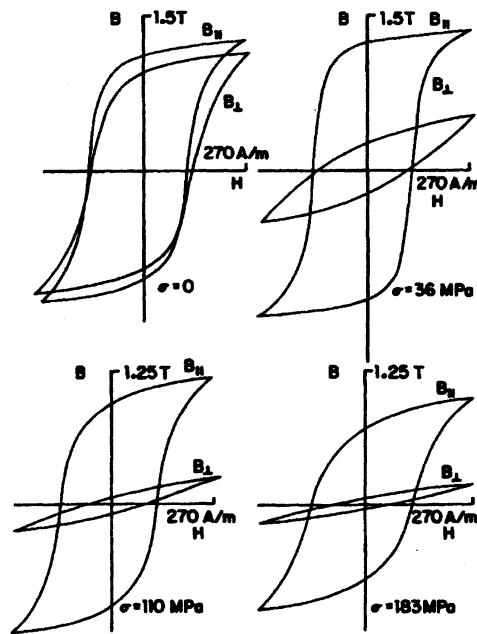


Figure 1.1. Changes in magnetic hysteresis of mild steel with an applied stress [2]

Magnetomechanical stress sensing material

The second stress detection method that has been developed also makes use of magnetic properties. This is a non-contact stress sensing material that utilizes the magnetomechanical effect for monitoring the amount of stress that is being applied to the

material. This method relies on applied stress to create some changes in magnetization as a result of magnetic domain wall motion within the material. By measuring the change in magnetization along a specific axis, the stress applied to the material can be determined. This magnetoelastic sensor material can be integrated into a mechanical system such as a rotating shaft or an aircraft wing. A remote field sensor such as a Hall effect device can be used monitor magnetization and hence the amount of stress being applied to the material.

Thesis Organization

The remaining parts of this thesis are organized into five additional chapters. Chapter 2 is a paper published by *IEEE Transactions on Magnetics* that presents a study of the Curie temperature of cobalt ferrite based composites for stress sensor applications. Chapter 3 is a paper submitted for publication to *Applied Physics Letters* that also covers a study on new manganese-substituted cobalt ferrite magnetostrictive materials for magnetic stress sensor applications. Chapter 4 contains a paper published in *Review of Progress in Quantitative Nondestructive Evaluation*, which describes the development of a magnetic non-destructive evaluation imaging system using magnetoresistive devices. Chapter 5 is a paper that has been accepted for publication in *IEEE Transactions on Magnetics* that covers the quantitative evaluation of stress distribution in magnetic materials by Barkhausen effect and magnetic hysteresis measurements. Chapter 6 presents the major conclusions of the research presented in this thesis.

References

1. Callister, William D. (2000) *Materials Science and Engineering An Introduction*, John Wiley & Sons, Inc.
2. Langman, R. (1985) IEEE Trans. Mag., 21, 1314

CHAPTER 2. STUDY OF CURIE TEMPERATURE OF COBALT FERRITE BASED COMPOSITES FOR STRESS SENSOR APPLICATIONS

Published by IEEE Transactions on Magnetics, 39, (5), 3316-3318, September, 2003.

J. A. Paulsen^{1,2,3}, C. C. H. Lo^{2,3}, J. E. Snyder^{3,4}, L. L. Jones, and D. C. Jiles^{2,3,4}

Abstract

Cobalt ferrite has been shown to be an excellent candidate for magnetic stress sensors due to a large magnetomechanical effect and high sensitivity to strain. However, near room temperature, the material exhibits some magnetomechanical hysteresis, which becomes negligible for temperatures of 60°C and above. Measurements indicate that doping the cobalt ferrite with silicon will lower the Curie temperature of the sensing material. It was also found that the Curie temperature of the material depends on the process that is used to produce the material. These results offer the possibility of decreasing the room temperature magnetomechanical hysteresis through adjusting the temperature dependence of magnetic and magnetomechanical properties.

¹Department of Mechanical Engineering,

²Center for Nondestructive Evaluation,

³Materials and Engineering Physics Program,

⁴Materials Science and Engineering Department, Iowa State University, Ames, Iowa, 50011, USA

Introduction

The development of new magnetoelastic materials for use in magnetic stress sensors is of scientific and technological interest due to the growing number of possible applications including automated control systems, non-contact torque sensing and imbedded stress-sensing applications. Most sensor applications require materials that exhibit large reversible changes in magnetization with applied stress or torque with minimal magnetomechanical hysteresis at ambient temperatures. In previous studies, metal bonded cobalt ferrite composites have been shown to be excellent candidates for stress sensors due to a large magnetomechanical effect and high sensitivity to strain. They show linear magnetostrictive strains of up to 225×10^{-6} with a $(d\lambda/dH)_{\max}$ of $1.3 \times 10^{-9} \text{ A}^{-1}\text{m}$ under no external load. They also show good mechanical properties, excellent corrosion resistance, and low cost [1-3].

Nevertheless they exhibit magnetomechanical hysteresis, and for these materials to be suitable for sensor applications, it is desirable to reduce this hysteresis. It was observed that the magnetomechanical hysteresis of toroid samples of metal-bonded cobalt ferrite composite became negligibly small at temperatures above 60°C (See Figure. 2.1) [2]. Therefore, the objective of this study is to investigate whether this temperature can be decreased by composition changes that decrease the Curie temperature of the ferrite, thus enabling operation within the temperature range of reversible magnetomechanical response.

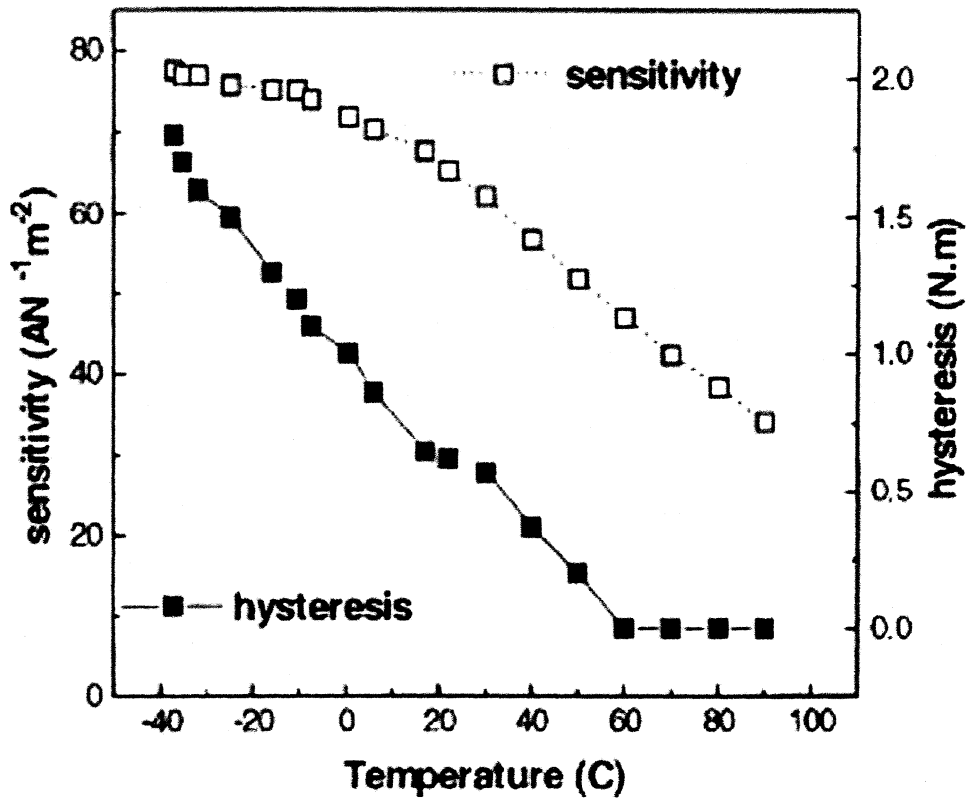


Figure 2.1. Variations in sensitivity (rate of change in surface magnetic field with applied torque) and magnetomechanical hysteresis of a metal-bonded cobalt ferrite composite (98 vol % $\text{CoO} \cdot \text{Fe}_2\text{O}_3$ + 2 vol % $\text{Ag}_{0.97}\text{Ni}_{0.03}$) toroid with temperature [2].

Materials

Varying Compositions

Silicon was identified as a possible candidate material for use in doping the cobalt ferrite material to lower the Curie point [4]. To investigate this possibility, a series of samples with compositions of $\text{Co}_{1+x}\text{Si}_x\text{Fe}_{2-2x}\text{O}_4$ (where x is 0 to 0.3) were prepared. The doped cobalt ferrite samples were made by mixing Fe_2O_3 , SiO_2 , and Co_3O_4 powders in the

targeted proportions and processed the following way: The powder was pressed and calcined at 1000°C for 24 hours, then ground and mixed by hand, and pressed and calcined again at 1000°C for 24 hours. The powder was then re-ground, mixed, pressed into slugs and sintered at 1250°C for 15 minutes. The samples were then rapid-cooled by removing from the furnace to room temperature air. Images of the samples were taken using a scanning electron microscope (SEM) to ensure the samples prepared were homogeneous and energy-dispersive x-ray spectroscopy (EDX) was used to determine the final composition of the samples. This procedure was repeated multiple times until the process of making the material was refined enough so as to get uniform homogeneous samples.

Varying Sintering Temperatures

To investigate whether the Curie temperature could be further altered by means of the process used to make the material, another set of five samples was prepared. The initial composition of these samples was $\text{Co}_{1.6}\text{Si}_{0.6}\text{Fe}_{0.8}\text{O}_4$ and the procedure for the sample preparation was the same as before except the powder was ground and mixed used a ball-milling method and the final sintering temperature was varied between 1050 °C and 1275 °C for the series of samples.

Experimental

The sample compositions were examined by EDX in an SEM to determine the actual composition after processing. This compositional analysis method could accurately measure the Co, Fe, and Si, but was unable to give accurate results for oxygen. To determine the Curie temperatures, the magnetic moment was measured as a function of temperature using a vibrating sample magnetometer (VSM) with a high temperature furnace and temperature controller, under computer control. The magnetic moment measurements were performed over a temperature range of 100°C to 650°C. The samples were heated up through the transition at a rate of 2°C per minute, then cooled back through the transition at the same rate. The cooling curves retraced the heating curves with no hysteresis in sensor temperature.

Curie temperatures were determined for each sample from the results of the VSM measurements. This was done by linearly extrapolating the magnetization vs. temperature curve from the region of maximum slope down to the temperature axis.

Results and Discussion

Varying Composition

VSM measurement results for the sample series with varying Si content are shown in Figure 2.2. EDX measurement results of the actual finished compositions of these samples are shown in the second column of Table 2.1 (the oxygen is shown as O_x, since oxygen

content could not be determined accurately by EDX). The third and fourth samples ended up after processing with more Co and Si, and less Fe than the initial percentages of starting material. The values determined for Curie temperature are shown in the third column of Table 2.1. One can see that substituting Si and Co for Fe in the series causes a decrease of Curie temperature, in the case of the fourth sample, by as much as 44°C.

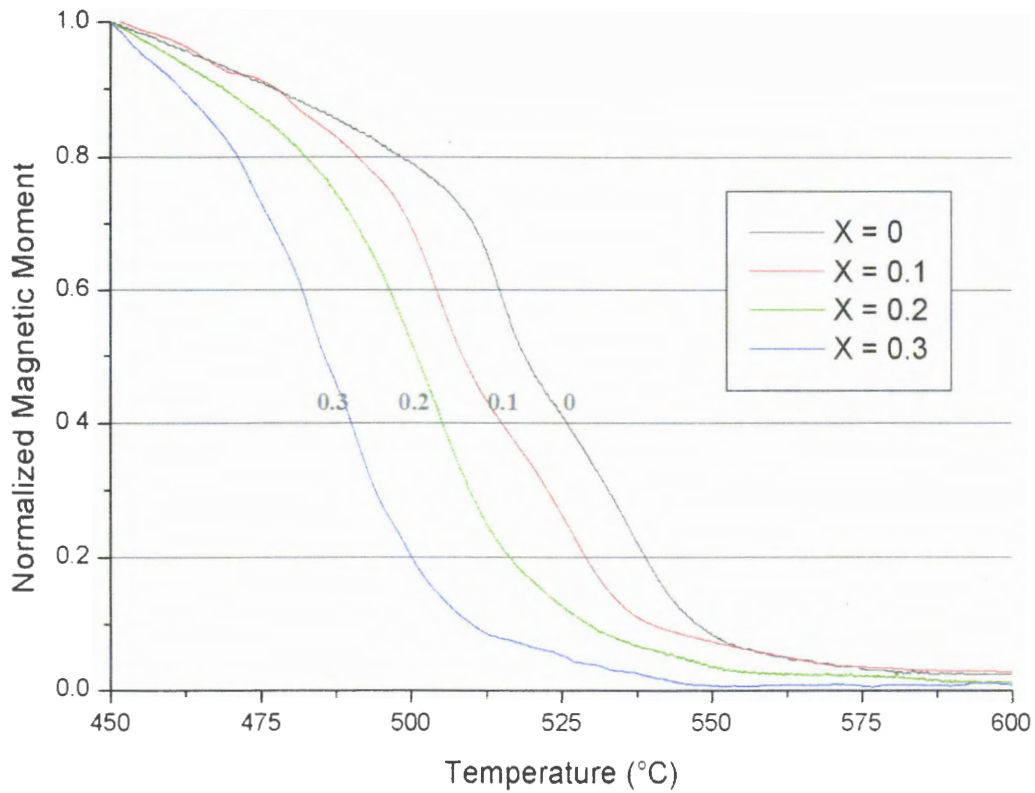


Figure 2.2. Normalized magnetic moment of Si-substituted cobalt ferrite as a function of temperature, for various Si contents

Table 2.1. EDX and VSM results for the series of Si-substituted Co-ferrite samples with varying amount of Si and Co substitution for Fe

| Initial Composition | Actual Finished Composition | Curie Temperature (°C) |
|---|--|------------------------------|
| CoFe_2O_4 | $\text{Co}_{1.1}\text{Fe}_{1.9}\text{O}_x$ | 552 |
| $\text{Co}_{1.1}\text{Si}_{0.1}\text{Fe}_{1.8}\text{O}_4$ | $\text{Co}_{1.11}\text{Si}_{0.08}\text{Fe}_{1.81}\text{O}_x$ | 535 |
| $\text{Co}_{1.2}\text{Si}_{0.2}\text{Fe}_{1.6}\text{O}_4$ | $\text{Co}_{1.42}\text{Si}_{0.31}\text{Fe}_{1.26}\text{O}_x$ | 521 |
| $\text{Co}_{1.3}\text{Si}_{0.3}\text{Fe}_{1.4}\text{O}_4$ | $\text{Co}_{1.67}\text{Si}_{0.47}\text{Fe}_{0.86}\text{O}_x$ | 508 |

The Curie temperature for pure cobalt-ferrite was determined to be 552°C, which is higher than that reported in Smit and Wijn (520°C) [5]. However our sample is cobalt-rich compared to stoichiometric CoFe_2O_4 (see Table 2.1). Furthermore we do not know how our thermal preparation temperatures, times, and cooling rates compare, and the site occupancy of Co and Fe among the A and B sites is known to depend on thermal treatment [6]. Thus one might expect Curie temperature differences.

The rate of decrease of Curie temperature with added Si content found in this study is considerably less than that found by Shinde and Hadhav [4]. However, thermal preparation conditions were considerably different: their final sintering was performed at 1050°C and the samples were slow-cooled at a rate of 2°C/min. In the current study, the samples were

sintered at 1250°C, then rapid-cooled by removing from the furnace to room temperature air. Site occupancy of the Co, Fe, and Si ions should depend on thermal treatment, since it is already known that site occupancy of Co and Fe in cobalt ferrite can depend on thermal treatment[6]. Furthermore, although the samples appear reasonably uniform in microstructure and composition in the SEM, we are still in the process of completing x-ray diffraction measurements that will tell us about possible secondary phases.

Varying Sintering Temperatures

VSM results for the series of samples with varying final sintering temperature are shown in Figure 2.3, and their finished actual compositions and Curie temperatures are shown in Table 2.2. The results for the samples sintered at 1050°C and 1150°C are essentially identical. However, for further increase in sintering temperature, the Curie temperature is found to decrease with increasing sintering temperature. Then for sintering temperatures of 1250°C and 1275°C, the Curie temperature changes only slightly. The overall change of Curie temperature from lowest to highest was 45°C.

Since the starting composition of these samples was identical and the actual finished compositions are very similar, it would appear that the different final sintering temperatures are changing the site occupancies of the Co, Fe, and Si among the A and B sites, and thus changing the details of the magnetic exchange coupling of the different sites, thus affecting the Curie temperature.

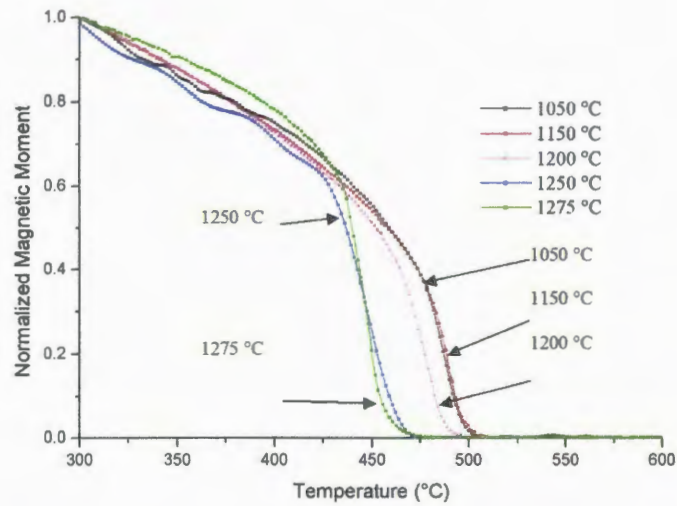


Figure 2.3. Normalized magnetic moment of Si-substituted cobalt ferrite vs. temperature, for various final sintering temperatures

Table 2.2. EDX and VSM results for the series of Si-substituted Co-ferrite samples with the same starting composition ($\text{Co}_{1.6}\text{Si}_{0.6}\text{Fe}_{0.8}\text{O}_4$), and different final sintering temperatures

| Sintering Temperature | Actual Finished Composition | Curie Temperature (°C) |
|-----------------------|--|------------------------|
| 1050 | $\text{Co}_{1.61}\text{Si}_{0.48}\text{Fe}_{0.91}\text{O}_x$ | 500 |
| 1150 | $\text{Co}_{1.60}\text{Si}_{0.50}\text{Fe}_{0.90}\text{O}_x$ | 500 |
| 1200 | $\text{Co}_{1.61}\text{Si}_{0.52}\text{Fe}_{0.88}\text{O}_x$ | 490 |
| 1250 | $\text{Co}_{1.57}\text{Si}_{0.46}\text{Fe}_{0.97}\text{O}_x$ | 458 |
| 1275 | $\text{Co}_{1.45}\text{Si}_{0.42}\text{Fe}_{1.13}\text{O}_x$ | 455 |

Conclusions

These results show that the Curie temperature of cobalt ferrite (CoFe_2O_4) can be adjusted over a substantial range by the substitution of Si and Co for Fe, and by a combination of Si, Co-substitution and varying thermal treatment. This suggests that the temperature dependence of magnetic and magnetomechanical properties can be adjusted by such substitutions and thermal treatments, in order to control the temperature dependence of magnetomechanical hysteresis. This could enable hysteresis-free sensor material operation at room temperature and offer a wide variety of new potential technological applications.

Acknowledgment

This work was supported by the National Aeronautical and Space Administration (NASA) through the Center for Nondestructive Evaluation at Iowa State University.

References

1. Y. Chen, J. E. Snyder, C. R. Schwichtenberg, K. W. Dennis, R. W. McCallum, D. C. Jiles, "Metal-bonded Co-Ferrite Composites for Magnetostrictive Torque Sensor Applications", *IEEE Trans. Magn.* vol. 35, p. 3652, 1999.
2. Y. Chen, J. E. Snyder, K. W. Dennis, R. W. McCallum, and D. C. Jiles, "Temperature-dependence of the magneto-mechanical effect in metal-bonded cobalt ferrite composites under torsional strain", *J. Appl. Phys.* vol. 87 p. 5789, 2000.
3. R. W. McCallum, K. W. Dennis, D. C. Jiles, J. E. Snyder, Y. H. Chen, *Low Temp. Phys.* vol. 27, p. 266, 2001.
4. S. S. Shinde and K. M. Jadhav, "Bulk Magnetic Properties of Cobalt Ferrite doped with Si^{4+} Ions", *J. Mat Sci. Lett.* Vol. 17, p. 849, 1998.
5. J. Smit and H. P. J. Wijn, *Ferrites: Physical Properties of Ferrimagnetic Oxides in Relation to their Technical Applications*, New York, John Wiley & Sons, 1959.
6. G. A. Sawatky, F. Van der Woude, and A. H. Morrish, *J. Appl. Phys.* vol. 39, p. 1204, 1996.

CHAPTER 3. NEW MANGANESE-SUBSTITUTED COBALT FERRITE MAGNETOSTRICTIVE MATERIALS FOR MAGNETIC STRESS SENSOR APPLICATIONS

A paper submitted for publication to Applied Physics Letters

J. A. Paulsen^{1,2,3}, A. P. Ring³, C. C. H. Lo^{2,3}, J. E. Snyder^{2,3,4} and D. C. Jiles^{2,3,4}

Abstract

Metal bonded cobalt ferrite composites have been shown to be promising candidate materials for use in magnetoelastic stress sensors, due to their large magnetomechanical effect and high sensitivity to stress. However below 60°C the cobalt ferrite material exhibits substantial magnetomechanical hysteresis. In the current study, measurements indicate that substituting Mn for some of the Fe in the cobalt ferrite can lower the Curie temperature of the material while maintaining a suitable magnetostriction for stress sensing applications. These results demonstrate the possibility of optimizing the magnetomechanical hysteresis of cobalt ferrite based composites for stress sensor applications, through control of the Curie temperature.

¹Department of Mechanical Engineering,

²Center for Nondestructive Evaluation,

³Materials and Engineering Physics Program, Ames Laboratory,

⁴Materials Science and Engineering Department, Iowa State University, Ames, Iowa 50011, USA

Introduction

Magnetostrictive cobalt ferrite composites hold promise for use in advanced magnetomechanical stress and torque sensors. Magnetoelastic stress sensors operate on the principle that magnetic properties of materials are altered by stress via the magnetoelastic coupling [1]. These magnetic property changes can be detected remotely, for example, by measuring magnetic field near the sensor surface using a Hall effect device [2]. Magnetoelastic materials therefore offer realistic prospects for development of contactless sensors for use in stress and torque applications.

Most stress sensor applications ideally require materials that exhibit large reversible changes in magnetization with applied stress together with minimal magnetomechanical hysteresis. In previous studies, metal bonded cobalt ferrite composites have been shown to be excellent candidates for stress sensors due to a large magnetomechanical effect and high sensitivity to stress. They show linear magnetostrictive strains of magnitude up to 225×10^{-6} with a rate of change of magnetostriction with applied field $(d\lambda/dH)_{\max}$ of up to $1.3 \times 10^{-9} \text{ A}^{-1}\text{m}$ under no external load. They also show good mechanical properties, excellent corrosion resistance, and low cost.[2-4]

A drawback to metal-bonded cobalt ferrite composite materials is that they exhibit some magnetomechanical hysteresis at room temperature, and for these materials to be suitable for sensor applications, it is desirable to reduce this hysteresis. It was observed that the magnetomechanical hysteresis became negligibly small at temperatures above 60°C [2].

Since the temperature dependence of magnetic and magneto-elastic properties is strongly influenced by the Curie temperature (T_C), the objectives of this study are to investigate whether T_C can be decreased through composition changes, while at the same time maintaining sufficient magnetostriction for stress sensor applications. This could enhance the reversible magnetomechanical response within the temperature range of interest and thereby allow control and reduction of magnetomechanical hysteresis.

In this work, manganese substituted cobalt-ferrite was fabricated and characterized to study the effects of composition on the Curie temperature and magnetostriction. Previous studies of Mn-substituted cobalt ferrite centered on thin films for magneto-optical applications and fine particles [5]. The effects of Mn on the magnetomechanical properties have not been reported. In the present study we report results of Curie temperature, magnetization, and magnetostriction for a series of sintered bulk Mn-substituted cobalt ferrite of composition $\text{CoMn}_x\text{Fe}_{2-x}\text{O}_4$ for $0 \leq x \leq 0.8$.

Experimental Procedures

A series of manganese-doped cobalt ferrite samples with compositions of $\text{CoFe}_{2-x}\text{Mn}_x\text{O}_4$ (where x ranges from 0 to 0.8) were prepared by substituting manganese for iron. The samples were made using standard powder ceramic techniques. The process involved mixing Fe_2O_3 , MnO_2 , and Co_3O_4 powders in the targeted proportions. The powder was calcined, ball-milled, mixed, and calcined again. The powder was then re-milled, mixed, pressed into slugs and sintered in air. The samples were cooled by removal from the furnace to room temperature. The microstructure of the samples was characterized using a scanning

electron microscope (SEM). Energy-dispersive x-ray spectroscopy (EDX) was used to determine the final composition of the samples. This fabrication procedure was refined until it produced uniform microstructures and chemically homogeneous samples. The compositions of the samples are given in Table 3.1.

Table 3.1. Target and final compositions for the series of manganese-doped cobalt ferrite samples with various amounts of manganese.

| Target Composition | Composition by EDX | | |
|--|--------------------|------|------|
| | Co | Fe | Mn |
| $\text{CoFe}_{1.8}\text{Mn}_{0.2}\text{O}_4$ | 0.95 | 1.83 | 0.22 |
| $\text{CoFe}_{1.7}\text{Mn}_{0.3}\text{O}_4$ | 0.98 | 1.73 | 0.29 |
| $\text{CoFe}_{1.6}\text{Mn}_{0.4}\text{O}_4$ | 0.95 | 1.62 | 0.44 |
| $\text{CoFe}_{1.4}\text{Mn}_{0.6}\text{O}_4$ | 0.93 | 1.43 | 0.65 |
| $\text{CoFe}_{1.2}\text{Mn}_{0.8}\text{O}_4$ | 0.96 | 1.2 | 0.84 |

To determine Curie temperatures, the magnetic moment was measured as a function of temperature using a vibrating sample magnetometer (VSM) with a high temperature furnace and temperature controller, under computer control. The magnetic moment measurements were performed over a temperature range of 100°C to 650°C. The samples were heated through the Curie temperature transition at a rate of 2 °C per minute, and then cooled back through the transition at the same rate. These measurements were performed

under an applied field of 8KAm^{-1} (100 Oe). Curie temperatures of the samples were determined from the cooling curves by linearly extrapolating the magnetic moment versus temperature curve from the region of maximum slope down to the temperature axis. Saturation magnetization of the samples was measured using the VSM under an applied field of 560KAm^{-1} (7 KOe).

Results and Discussion

The temperature dependence of the normalized magnetic moment of the pure cobalt ferrite and the material with various amounts of manganese substituted for Fe is shown in Figure 3.1. All of the samples exhibited a sharp increase in magnetic moment on cooling through the Curie temperature. It is evident that substituting Mn for Fe in cobalt ferrite reduced the Curie temperature, by as much as 300°C in the case of $\text{CoFe}_{1.2}\text{Mn}_{0.8}\text{O}_4$.

Figure 3.2 shows the saturation magnetization of pure cobalt ferrite along with the Mn-substituted ferrite samples at room temperature. Although Mn substitution made a substantial decrease in Curie temperature, saturation magnetization showed only a modest decline (maximum of 20% over the range of $0 \leq x \leq 0.8$).

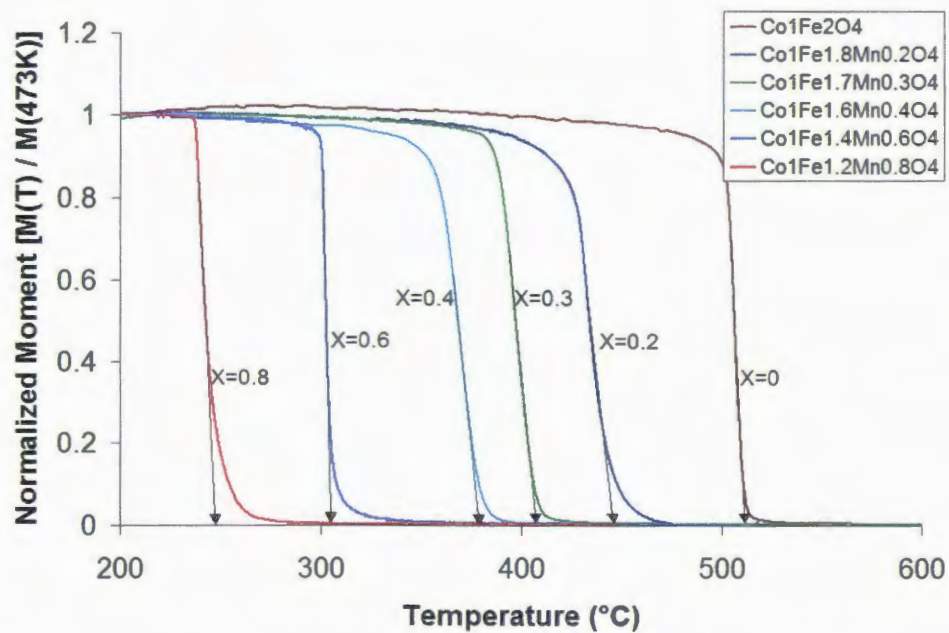


Figure 3.1. Normalized magnetic moment versus temperature upon cooling for pure cobalt ferrite and manganese-doped cobalt ferrite

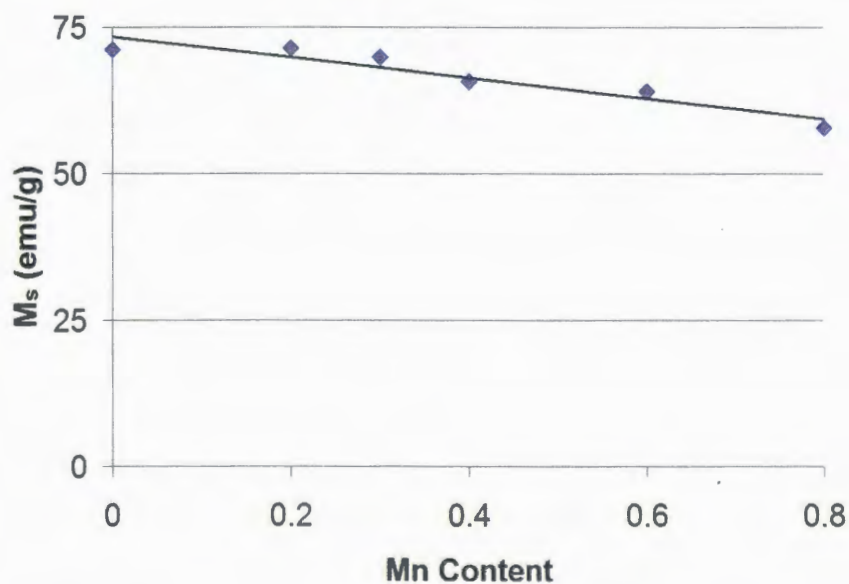


Figure 3.2. Saturation magnetization of manganese-substituted cobalt ferrite $\text{CoFe}_{2-x}\text{Mn}_x\text{O}_4$ with various manganese contents at room temperature. The applied field was 560 KAm⁻¹ (7000 Oe).

As shown in Figure 3.3, samples with low manganese contents (e.g. $\text{CoFe}_{1.8}\text{Mn}_{0.2}\text{O}_4$) have saturation magnetostriction comparable with that of pure cobalt ferrite. Further increase in manganese content reduces the saturation magnetostriction. It should however be noted that even the lowest saturation magnetostriction (55 ppm for $\text{CoFe}_{1.2}\text{Mn}_{0.8}\text{O}_4$) is higher than that of nickel which in the past has been considered for magnetomechanical sensors [6]. Furthermore, Mn substitution does not appear to adversely affect the slope of the magnetostriction curve ($d\lambda/dH$) at low field. This slope is related to the stress sensitivity [7] and is an indication of potential performance of a magnetomechanical sensor based on this material.

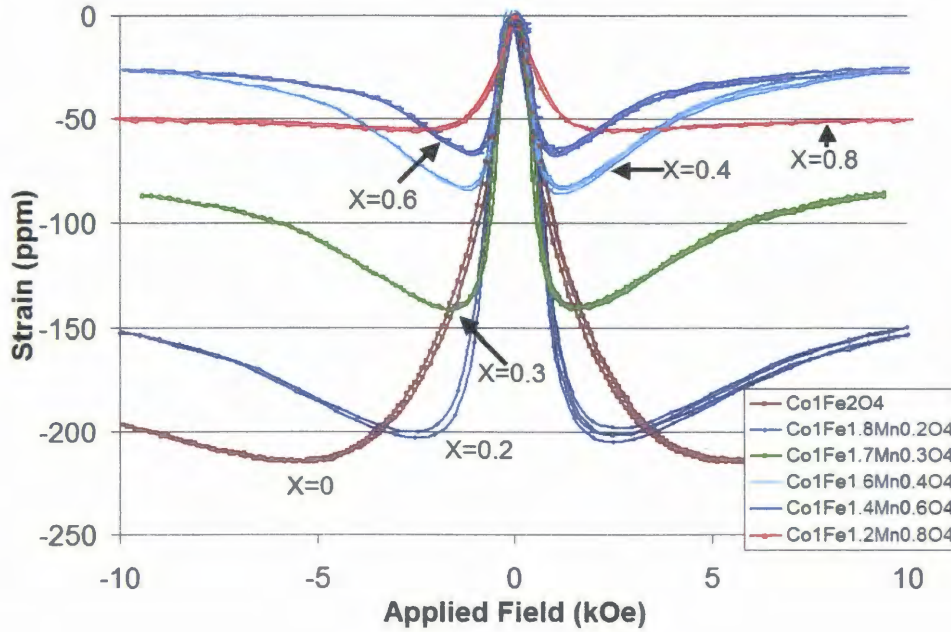


Figure 3.3. Magnetostriction curves for manganese-doped cobalt ferrite samples.

The Curie temperature decreases approximately linearly with increasing manganese content as shown in Figure 3.4. When the Mn content increases, the magnitude of the maximum magnetostriction also decreases as a function of Mn content.

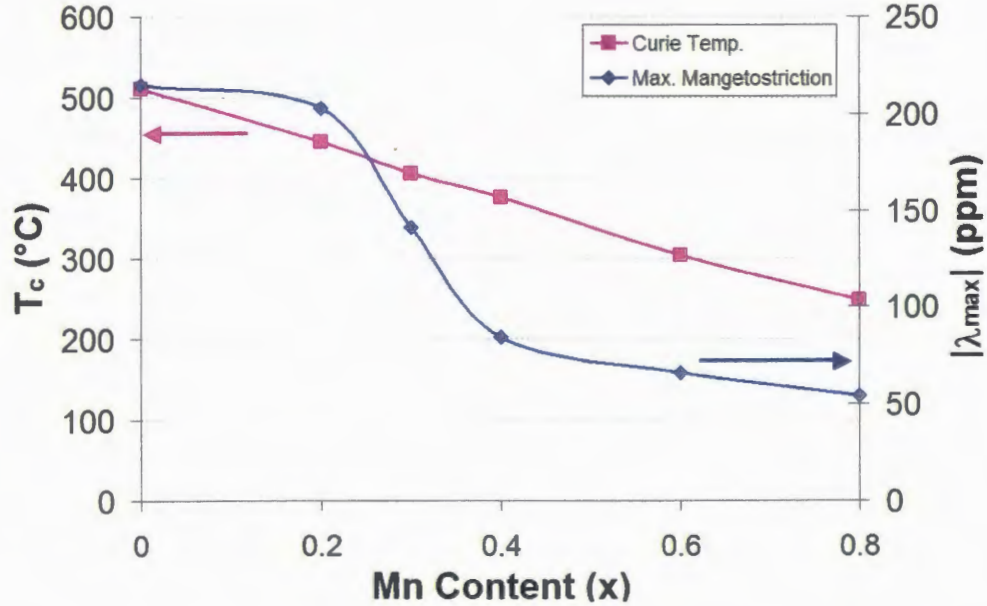


Figure 3.4. The Curie temperature and magnitude of maximum magnetostriction $|\lambda_{\text{max}}|$ of the manganese-doped cobalt ferrite samples versus the manganese content.

These results indicate that manganese-substituted cobalt ferrites offer improved scope for developing magnetomechanical sensors and actuators beyond that possible with the original cobalt ferrite material. Substitution of Mn for Fe has the effect of making substantial decrease in Curie temperature, which should have a substantial effect on the temperature dependence of magnetic and magnetomechanical properties contributing to magnetomechanical hysteresis. The maximum magnetostriction magnitude, although decreased as a result of the Mn additions, is still sizeable, and should be more than sufficient

for use as a magnetomechanical stress sensing material for many applications. Saturation magnetization, upon which the magnitude of the external field used in non-contact sensing will depend, shows only a modest decrease throughout the compositional range. Similarly, the slope of the magnetostriction curve at low field, upon which the sensitivity for stress sensing applications depends, does not appear to be adversely affected. Thus it should be possible to adjust the temperature dependence of magnetomechanical hysteresis while still maintaining sufficient magnetomechanical sensor material performance.

Conclusions

The effects of composition on the magnetic and magnetomechanical properties of cobalt ferrite doped with manganese have been studied. The results show that the Curie temperature of cobalt ferrite can be reduced over a substantial range by the substitution of Mn for Fe. The fact that the Curie temperature and magnetostriction of manganese-doped cobalt ferrite are selectable by adjusting manganese content allows the material properties to be optimized for use as stress sensors over a range of operational temperatures.

Acknowledgments

This research was supported by the National Aeronautical and Space Administration (NASA) under award No NAG-1-02098.

References

1. D. C. Jiles, *J. Phys. D: Applied Physics*, 28, 1537 (1995).
2. Y. Chen, J. E. Snyder, C. R. Schwichtenberg, K. W. Dennis, R. W. McCallum, D. C. Jiles, *IEEE Trans. Magn.* 35, 3652 (1999).
3. Y. Chen, J. E. Snyder, K. W. Dennis, R. W. McCallum, and D. C. Jiles, *J. Appl. Phys.* 87, 5789 (2000).
4. R. W. McCallum, K. W. Dennis, D. C. Jiles, J. E. Snyder, Y. H. Chen, *Low Temp. Phys.* 27, 266 (2001).
5. B. Zhou, Y. Zhang, C.S. Liao, F.X. Cheng, C.H. Yan, L.Y. Chen, S.Y. Wang, *App. Phys. Lett.*, 79(12), 1849 (2001).
6. I.J. Garshelis, "Magnetic and mechanical material requirements for magnetoelastic torque transducers", 5th Conference on Magnetic Materials Measurements and Modeling (5M⁴), May 16 - 17, 2002, Iowa State University, Iowa, USA.
7. Y. Chen, B.K. Kriegermeier-Sutton, J.E. Snyder, K.W. Dennis, R.W. McCallum, D.C. Jiles, *J. of Magnetism and Magnetic Materials*, 236(1-2), 131 (2001).

CHAPTER 4. DEVELOPMENT OF A MAGNETIC NON-DESTRUCTIVE EVALUATION IMAGING SYSTEM USING MAGNETORESISTIVE DEVICES

Published in Review of Quantitative Nondestructive Evaluation, Vol. 22, p 931-938, 2003

C. C. H. Lo^{2,3}, J. A. Paulsen^{1,2,3}, and D. C. Jiles^{2,3,4}

Abstract

A magnetic imaging system has been developed for non-destructive evaluation of structural and mechanical conditions of materials using magnetic hysteresis and Barkhausen effect (BE) measurements. The system can be used to measure magnetic properties while scanning the surface of a material, and to convert the data into an image showing variations in the material conditions from one location to another. An integrated sensor probe capable of measuring both magnetic hysteresis and BE signals was developed using magnetoresistive devices. The imaging system has been found useful in detecting surface and sub-surface notches as well as thickness variations in steel plates.

¹Department of Mechanical Engineering,

²Center for Nondestructive Evaluation,

³Materials and Engineering Physics Program,

⁴Materials Science and Engineering Department, Iowa State University, Ames, Iowa 50011, USA

Introduction

We have developed a magnetic imaging system for non-destructive evaluation of structural and mechanical conditions of materials through magnetic hysteresis and Barkhausen effect measurements. The mechanical properties of materials deteriorate when their structure changes as a result of cyclic or excessive stresses, loading at elevated temperatures or impact damage. The degradation processes such as fatigue and creep involve cumulative, localized changes in both structure and stress state of materials which are often difficult to detect until the materials near the end of their lifetime. Failure of materials may occur without any significant change in macroscopic appearance in the material. Prior knowledge of the state of damage on a microscopic scale and its accumulation rate is therefore essential to determine the approach to failure.

Magnetic measurement techniques such as hysteresis loop and Barkhausen effect have been established through prior research as viable techniques for evaluating performance-related properties of materials [1]. Traditional empirical approaches, using magnetic measurements on bulk materials, involve detecting magnetic signals that represent averaged responses of the volume of the materials interrogated by an applied field [2]. Although this approach has proved promising in detecting degradation of the material condition as a whole, it may not be sufficient to reveal accumulation of material damages such as those induced by fatigue or creep, which are in general highly localized.

To fully exploit the potential of magnetic measurement methods for material evaluation we have developed a magnetic NDE imaging system that can be used to inspect

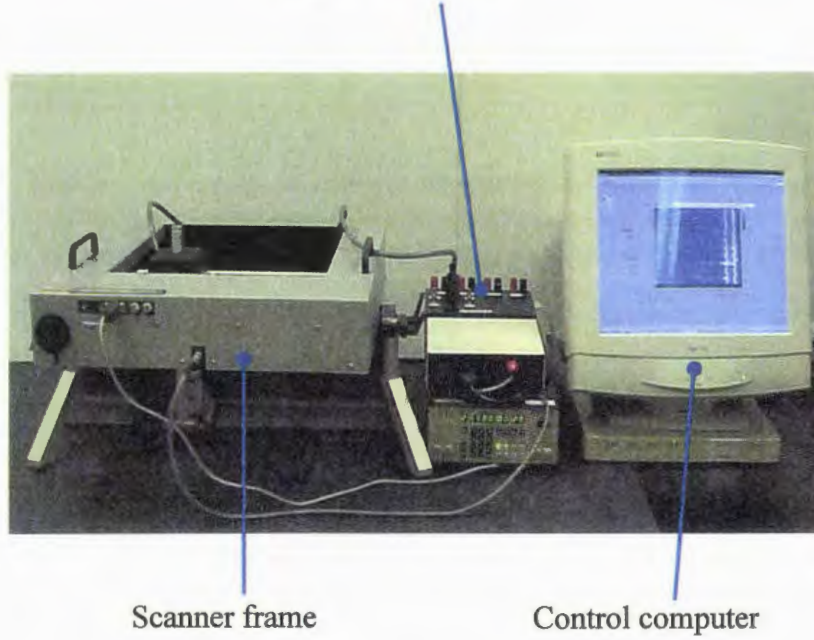
variations in material conditions. The approach is based on the fact that magnetic and mechanical properties of materials are closely related via the magnetoelastic coupling [3]. By imaging the magnetic properties of a sample, an image of the sample's mechanical properties can be obtained because of the magnetoelastic coupling. This can be used to identify localized material damages that are prone to failure. A similar approach has been adopted by Altpeter *et al* in the development of a Barkhausen microscope for evaluating material conditions through imaging Barkhausen effect signals [4].

The magnetic imaging system developed in this work is capable of scanning the surface of a material while measuring magnetic properties using a surface sensor. In order to obtain both high sensitivity and spatial resolution a new sensor probe was constructed using giant magneto-resistive (GMR) devices for detecting magnetic signals. Magnetoresistive sensors have been used in other studies for investigating grain structure and anisotropy in steel sheets through imaging of magnetic domains [5,6]. In this study GMR devices were used since they offered high field sensitivity, wide bandwidth, small size and low power consumption. A software package was developed for controlling the scanning process, acquiring and analyzing detected magnetic signals, and converting the measured magnetic properties into images that show the variations in material conditions from one location to another. The magnetic imaging system has been found capable of detecting surface notches as small as 0.25 mm wide and sub-surface notches which are 6 mm below the material surface, showing that the system provides a useful NDE tool for imaging conditions of materials, and for detecting defects that threaten integrity of engineering components.

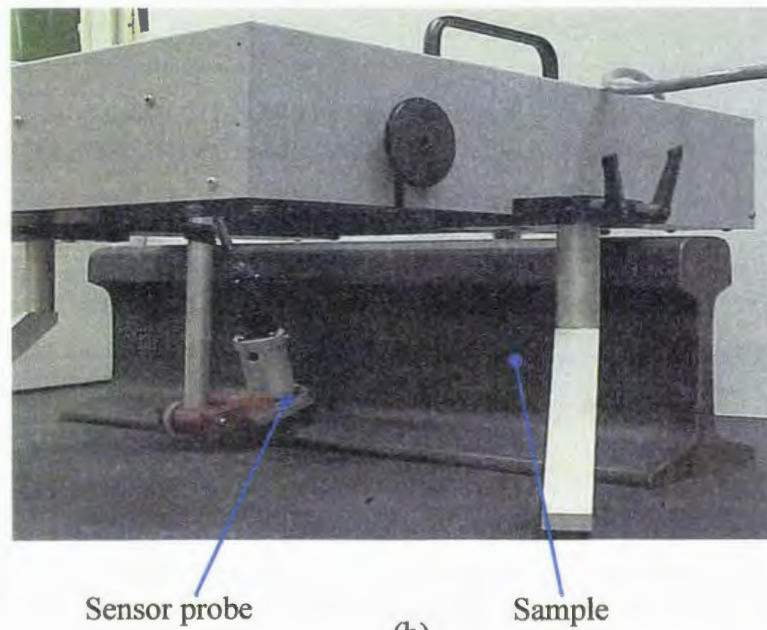
Magnetic Imaging System

The magnetic imaging system developed in this work is shown in Figure 4.1. It consists of a portable stepper-motor driven x-y scanning frame (Model: XT-3600 Plus, Xactec Corp.) and a signal processing module which are both controlled using a personal computer. During the scanning process the sample under test remained stationary while a sensor probe was raster scanned over the sample surface. The minimum step size is 0.025 mm and the largest scan size is 250 mm by 250 mm. A specially designed manipulator was used to ensure repeatable coupling between the sensor probe and the sample.

An integrated magnetic sensor probe was constructed that can be used to measure both magnetic hysteresis and Barkhausen signals. The schematic diagram of the sensor probe is shown in Figure 4.2. It consists of an electromagnet for applying a magnetizing field to a test specimen. Magnetic induction signals were detected using an inductive coil, while the tangential magnetic field at the sample surface was measured using an InSb Hall effect element (Model: HW-302B, Asahi Kasei Electronics, Japan) which offered a higher field sensitivity (7 mV/Oe.V) than GaAs Hall elements (30 μ V/Oe.V). The outputs of both the flux coil and the Hall effect element were amplified by factors of $\times 12$ and $\times 20$ respectively using wide-band differential amplifiers to improve the signal-to-noise ratio.

Signal processing

(a)



(b)

Figure 4.1. (a) The magnetic scanning system. (b) Scanning in progress.

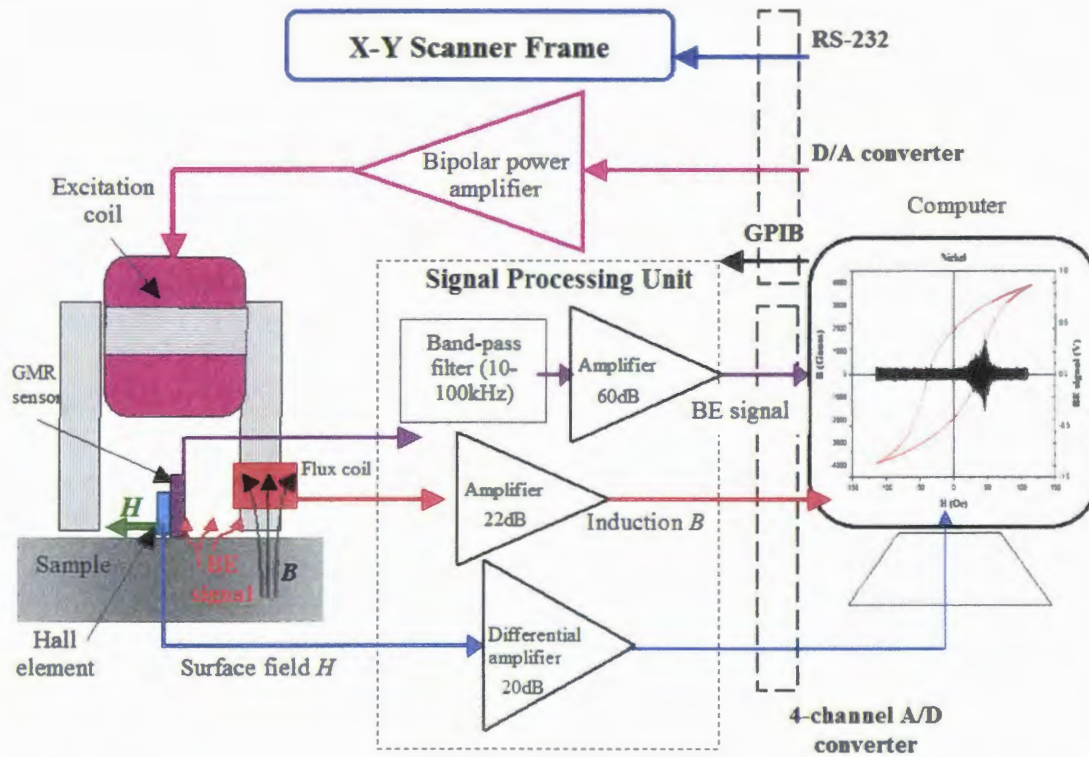


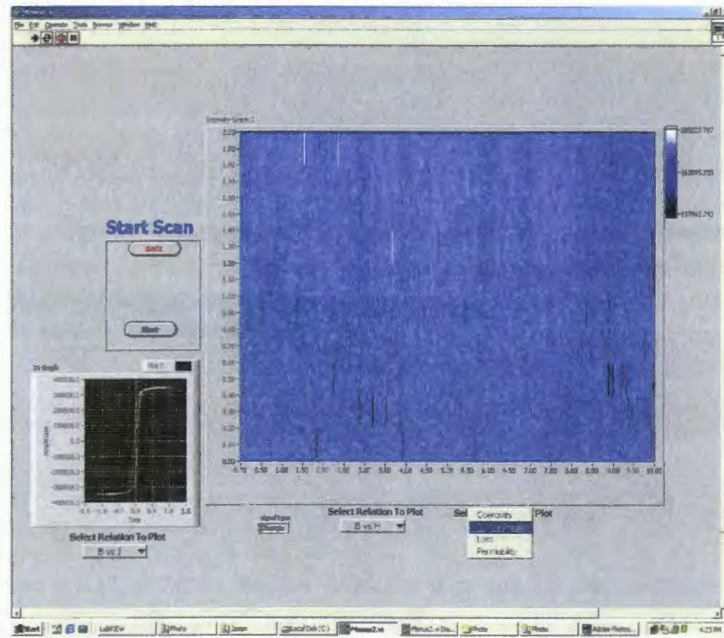
Figure 4.2. Schematic diagram of the magnetic imaging system.

A giant magnetoresistive (GMR) device (Model: AB005-01, Non Volatile Electronics, Inc.) was incorporated into the sensor probe for detecting Barkhausen effect signals emanating from the sample surface. The GMR sensor output was first amplified (voltage gain = 20 dB) and then filtered using a high-pass filter (cut-off frequency = 10 kHz) to remove the low-frequency component. The filtered signal was further amplified by 40 dB and was then low-pass filtered (cut-off frequency = 100 kHz) to reduce the electronic noise. With the use of the bandpass filter BE signals down to 1.5×10^{-4} G can be detected. It was noticed that the output of the GMR device exhibited non-linear and hysteretic responses to applied field in the low field regime (below 10 Oe). A possible way to alleviate this problem is to bias the device so that the device operated in the linear regime. The processed magnetic

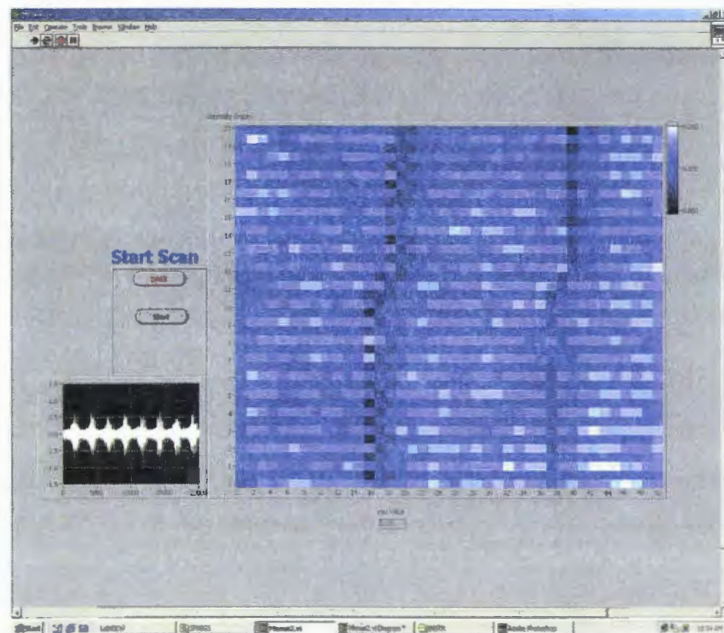
field, induction and Barkhausen effect signals were stored in a desk top computer using a 4-channel, 12-bit analog-to-digital (D/A) converter capable of sampling data up to 10 MHz.

The functionalities of the magnetic scanning system derive largely from the computer software package developed in this work. Several routines were incorporated into the software for measuring hysteresis loop and BE signals while scanning a sample. They provide the users complete control of the scanning processing (e.g. scan size and step size), measurement conditions (e.g. waveform, amplitude and frequency of magnetizing field signal), signal processing (e.g. filter settings) and data acquisition and analysis (e.g. sampling rate).

The hysteresis measurement routine performs real-time analysis of the measured hysteresis loop to extract magnetic properties such as coercivity, remanence, maximum permeability and hysteresis loss, which can be plotted as a function of the probe position to form two dimensional images (Figure 4.3 (a)). It also carries out harmonic analysis on the hysteresis data to determine the harmonic components, which have been shown in previous research to be sensitive to stress and microstructure of steel [7]. The Barkhausen effect routine allows users to specify the measurement conditions such as the excitation field signal, filter settings (passband and voltage gain), sampling rate and number of magnetization cycles of data acquisition. It also determines the root-mean-square (rms) values of the acquired BE signals for constructing images of the sample surface (Fig. 4.3 (b)), and performs fast Fourier transform (FFT) on the data.



(a)



(b)

Figure 4.3. Software interfaces of the (a) magnetic hysteresis measurement routine and (b) Barkhausen effect measurement routine showing the acquired hysteresis and BE signals (insets) and the corresponding two dimensional images (in blue) obtained from a steel plate with surface notches.

Experimental studies using the magnetic scanning system

The performance of the magnetic imaging system for NDE applications has been evaluated in a series of experimental studies. These included detection of surface notches, reverse-side notches and thickness variations.

Detection of Surface Notches

One application of the magnetic imaging system is to detect surface discontinuities such as fatigue cracks that threaten the integrity of engineering structures. The technique relies on the fact that any surface discontinuities in magnetic materials subjected to an applied field disrupt the local field distribution, and therefore are manifested as anomalies in the images of the detected magnetic hysteresis and Barkhausen effect signals.

To evaluate the feasibility of detecting surface cracks using the magnetic scanning system, magnetic hysteresis and Barkhausen scans were obtained from a notched plain carbon steel plate. Surface notches with depths of 1 mm and 2 mm and various widths ranging from 0.25 mm to 1 mm were cut using an electric discharge machine (EDM). During the experiments the sensor probe was scanned over an area of 178 mm \times 76.2 mm of the sample in steps of 1.25 mm. The probe remained stationary when measuring hysteresis loop and Barkhausen effect signals, which took about 12 and 1 second respectively. The sample was demagnetized at each scanning step prior to conducting hysteresis loop measurements.

The results of the Barkhausen scans are shown in Figures 4.4 and 4.5. All the surface notches are visible as stripes in the two dimensional image of the rms value of BE signals (Figure 4-4). The contrast (colour depth) is in general stronger for wider and deeper notches. This is evident in a higher resolution Barkhausen scan of the 1 mm wide notches (Figure 4-5), in which the deeper notch (on the left) shows a stronger contrast.

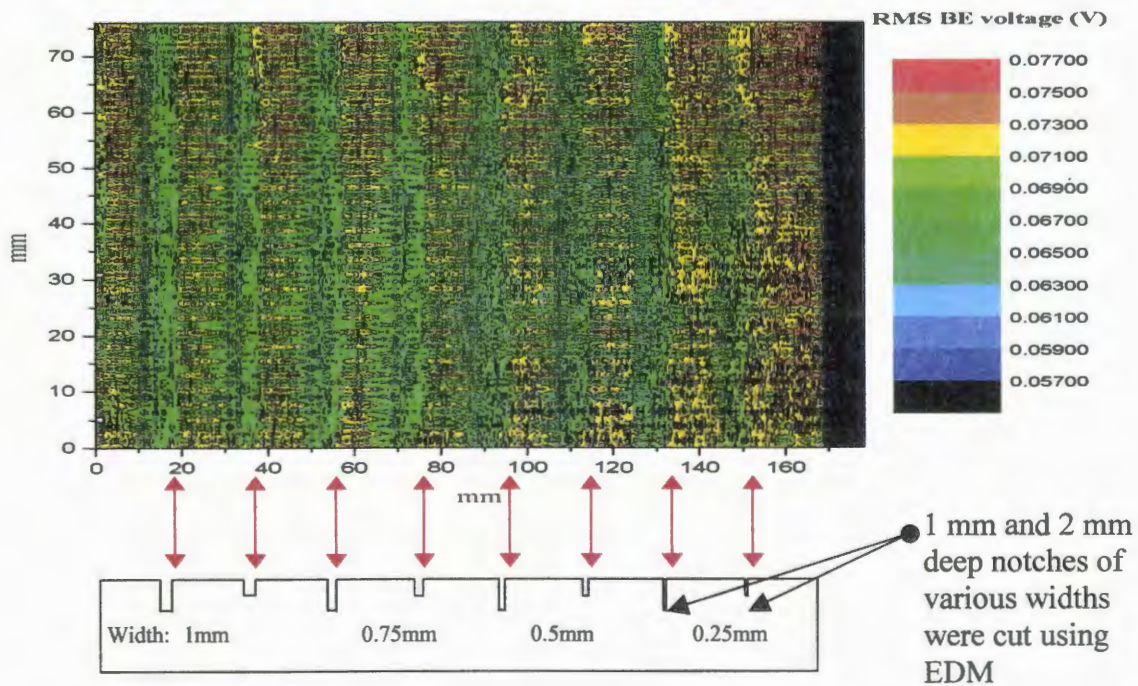


Figure 4-4. Scanned image of the rms values of Barkhausen effect signal measured from the plain carbon steel plate with surface notches.

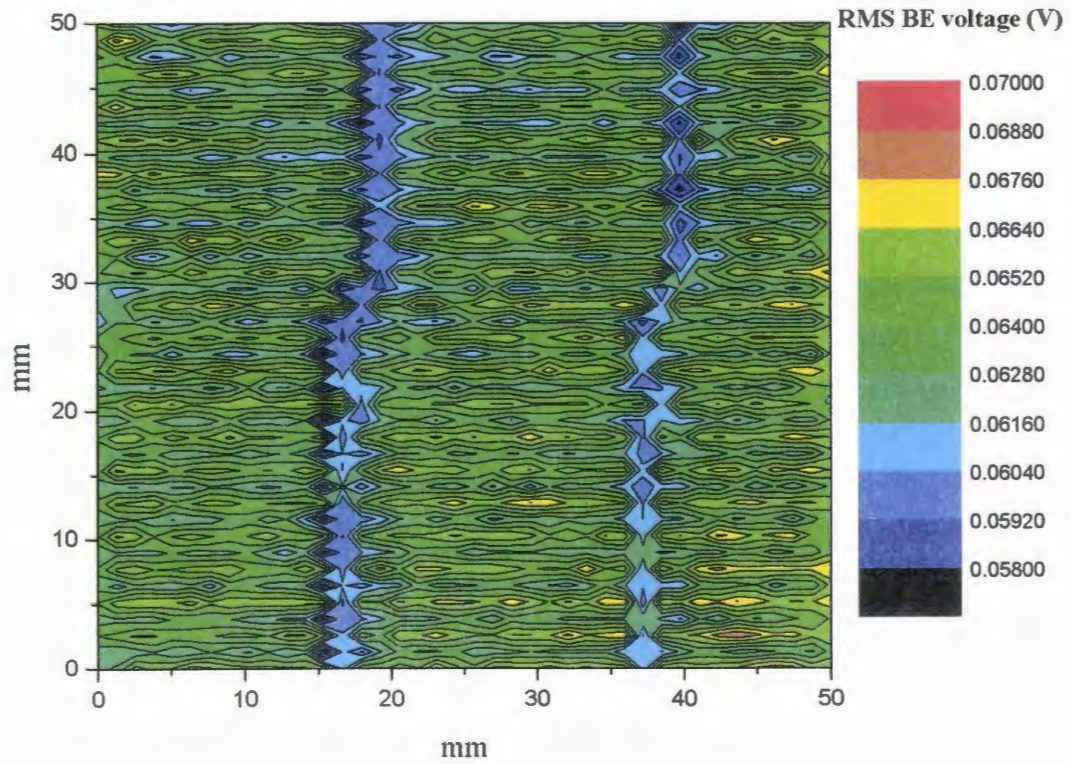


Figure 4-5. High resolution Barkhausen scan of the 1 mm wide surface notches in the steel plate.

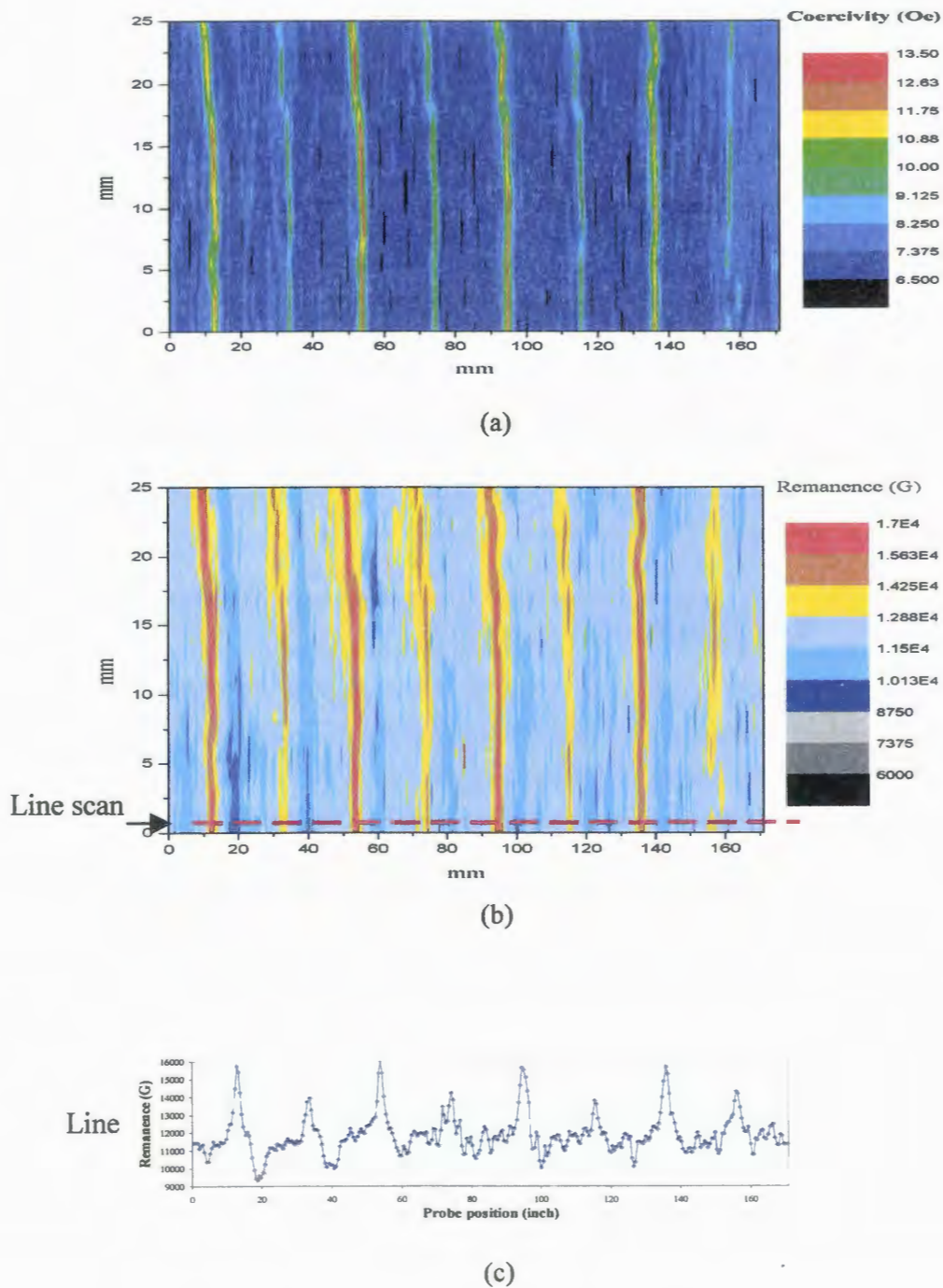


Figure 4-6. Scanned (a) coercivity and (b) remanence images of the carbon steel plate with surface notches. The difference in contrast between the shallow and deep notches is evident in the line scan of the remanence values shown at the bottom.

As shown in Figure 4-6, all the notches are well delineated in the images of hysteresis loop properties such as coercivity and remanence. In general the notch images obtained in the hysteresis loop scan are sharper than those observed in the Barkhausen scan images. Similar to the Barkhausen scan results, deeper notches show strong contrast than shallower ones. This is shown in the line scan of the remanence image (at the bottom of Figure 4-6(b)), in which the 2 mm deep notches consistently give rise to higher remanence values than the 1 mm deep notches with the same width.

Detection of Reverse-Side Notches

It is of practical interest to monitor material thickness or to detect cracks on inner walls of engineering components such as steel containers while only the outer surface is accessible. Magnetic measurements are promising techniques for addressing these NDE problems, since any thickness variation or the presence of cracks in an otherwise homogeneous structure disrupts the magnetic field distribution and this can be detected by imaging the magnetic properties of the materials. It was expected that magnetic hysteresis measurements are more suitable than Barkhausen effect measurements for detecting bulk conditions of material, since for hysteresis measurements the detected magnetic induction and field signals represent the averaged responses of the volume of the sample which is interrogated by the applied field, while for Barkhausen measurement the detected signal comes primarily from the surface layer of the sample as those generated deep inside the sample are greatly attenuated due to eddy current shielding.

The sample used in this study was an AISI 1020 plain carbon steel plate, which was machined using an EDM to produce sections with different thicknesses. Semi-circular grooves with various radii (from 2.5 mm to 6 mm) and 2.5 mm wide rectangular notches with different depths (from 2.5 mm to 6 mm) were cut into the bottom side of the steel plate using the EDM. Images of hysteresis loops were obtained by scanning the sensor probe over the top surface of the steel plate.

Most of the notches and grooves in the steel plate can be detected in the scanned images of hysteresis loop properties including maximum permeability, coercivity and remanence. As shown in Figure 4-7, the notches and grooves in the thinnest section show the strongest contrast in the permeability image. They were also clearly observed in the scanned images of coercivity and remanence as shown in Figure 4-8. In contrast to the permeability image, both coercivity and remanence were found to exhibit lower values around the defects. Contrast was observed between the regions with different thicknesses (5 mm and 7.5 mm) in the scanned permeability, coercivity and remanence images (Figures 4-7 and 4-8), suggesting that the technique can also be used to detect thickness variations in steel plates.

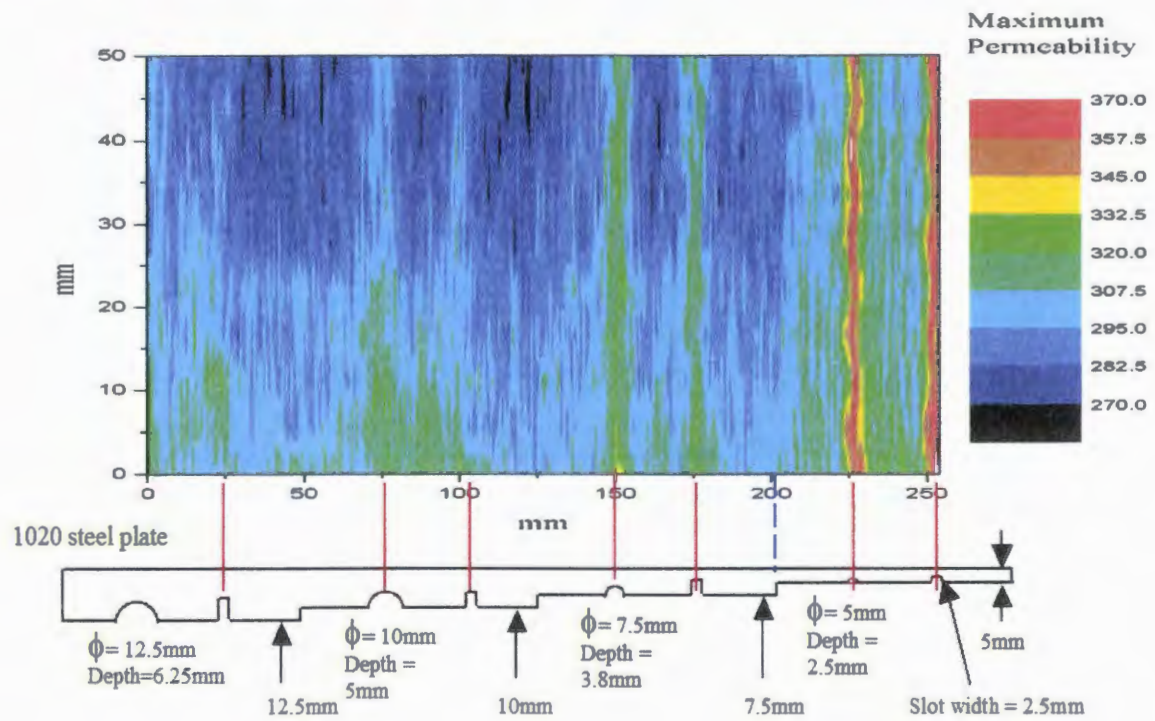
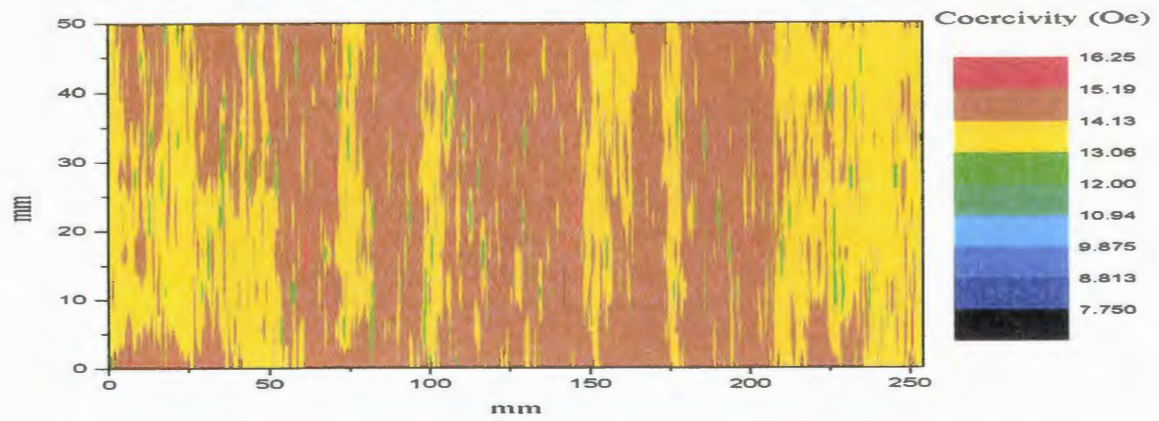
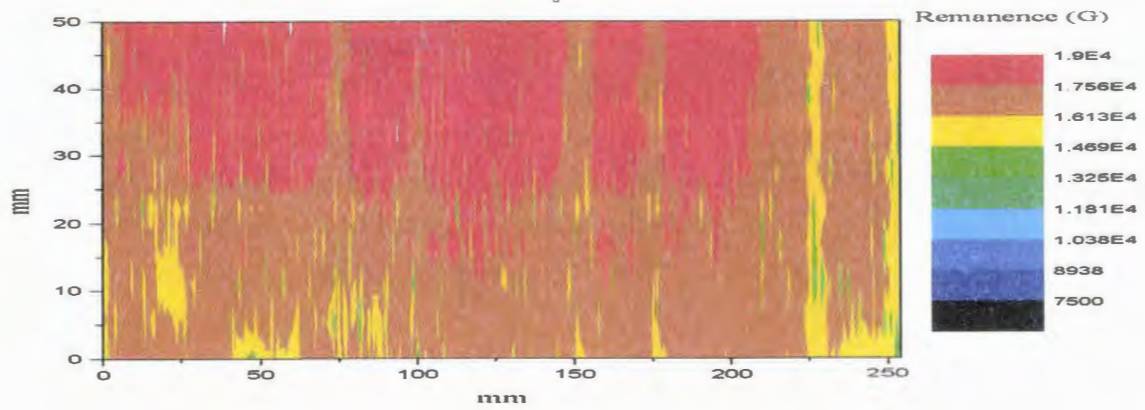


Figure 4-7. Image of the maximum permeability obtained from the 1020 steel plate.



(a)



(b)

Figure 4-8. (a) Coercivity and (b) remanence images showing the sub-surface notches and thickness variations in the 1020 steel plate.

Acknowledgements

This work was supported by the NSF Industry/University Cooperative Research Program at the Center for Nondestructive Evaluation and by the SPRIGS 2002 Grant from Iowa State University.

References

1. D. C. Jiles, "Magnetic methods in nondestructive testing", D.C.Jiles, (Invited paper), *Encyclopedia of Materials Science and Technology*, p. 6021. Ed. K.H.J. Buschow *et al.*, Elsevier Press, Oxford, September 2001.
2. M. J. Johnson, C. C. H. Lo, B. Zhu, H. Cao and D. C. Jiles, "Magnetic Measurements for NDE: Background, Implementation and Applications", (Invited paper), *Journal of Non destructive Evaluation*, Vol. 20, issue 4, pp 11-22, December 2000.
3. D. C. Jiles, "Theory of the magnetomechanical effect", *J. Phys. D: Applied Physics*, 28, 1537, 1995.
4. Altpeter, G. Dobmann, S. Fabender, J. Hoffmann, J. Johnson, N. Meyenndorf and W. Nichtl-Pecher, "Detection of residual stresses and modular growth in thin ferromagnetic layers with Barkhausen and acoustic microscopy", *Nondestructive Characterization of Material VIII*, p. 677, Ed. R.E. Green Jr. Plenum Press, NY, 1998.
5. P.I. Nicholson, "Nondestructive surface inspection system of steel and other ferromagnetic materials using magnetoresistive sensors", *J. Magn. Magn. Mat.* 160, 162-164, 1996.

6. S. Tumanski, Magnetovision, *McGraw Hill 2000 Yearbook of Science and Technology*, 242-244, 1999.
7. S.N.M. Willcock and B.K. Tanner, "The application of harmonic analysis to the magnetic properties of high-tensile steels", *Mater. Lett.*, 4(5,6,7), 307-312, 1986.

CHAPTER 5. QUANTITATIVE EVALUATION OF STRESS DISTRIBUTION IN MAGNETIC MATERIALS BY BARKHAUSEN EFFECT AND MAGNETIC HYSTERESIS MEASUREMENTS

Accepted for publication in IEEE Transaction on Magnetics, 2004

C. C. H. Lo^{2,3}, J. A. Paulsen^{1,2,3}, E.R. Kinser^{3,4}, and D. C. Jiles^{2,3,4}

Abstract

The feasibility of determining surface stress distribution in magnetic materials by magnetic measurements has been studied using a newly developed magnetic imaging system. The results indicate that magnetic measurements can be used for detecting stress concentration in magnetic materials non-destructively. The system measured hysteresis loop and Barkhausen effect signal using a surface sensor, and converted the data into a two-dimensional image showing spatial variations in magnetic properties. The sample used in this study was a nickel plate machined into a shear stress load beam configuration. When compressive stresses were applied along the neutral axis of the sample, the image of

¹Department of Mechanical Engineering, Iowa State University,

²Center for Nondestructive Evaluation, Iowa State University,

³Materials and Engineering Physics Program, Ames Laboratory,

⁴Materials Science and Engineering Department, Iowa State University, Ames, Iowa 50011, USA

magnetic properties such as coercivity exhibited patterns which were similar to the stress distributions calculated using finite element model (FEM). For direct comparison with FEM results, stress distributions were determined empirically from the measured coercivity values using experimental calibration of the stress dependence of coercivity. The stress patterns derived from the measured magnetic properties were found to closely resemble those calculated using FEM.

Introduction

There has been increasing demand for nondestructive evaluation (NDE) techniques for monitoring residual stress profiles in surface-treated components such as shot-peened or case-hardened steels, in which a compressive residual stress is usually induced in the surface layer to help retard fatigue crack growth. After extended service, the residual stress profiles of these components could change significantly as a result of degradation processes such as fatigue or creep, or stress release that occurs when the components are used at elevated temperatures. Non-invasive stress measurements become essential to exploiting the beneficial effects of surface treatment, since residual stress profiles are needed for predicting impending failure of critical components.

Currently, x-ray diffraction is the most reliable technique for residual stress assessment. The technique is however limited to probing a thin surface layer (tens of

microns), which is about an order of magnitude thinner than the typical penetration depth of residual stress induced by surface treatments. Magnetic methods such as hysteresis measurement offer an attractive technique for detecting stress profile in bulk materials. It has been established in previous work that the mechanical condition of magnetic materials, such as the residual stress state, strongly affects the magnetic properties via the magnetomechanical coupling [1]. Therefore stress or microstructural variations can be monitored from the data obtainable from magnetic measurements [2-5]. In this work the potential of magnetic measurement methods for detecting stress distribution in materials was evaluated with the use of a recently developed magnetic imaging system [6]. The system measures the spatial variations of magnetic properties nondestructively by scanning a sensor probe over the material surface. The image of the surface obtained by mapping the spatial variations of magnetic properties, contains information about the stress concentrations because of the magnetoelastic coupling.

Experimental details

The sample used in this study was a 6.4 mm thick, cold-worked nickel plate which was machined using an electric discharge machine (EDM) into a shear-beam load cell configuration as shown in Figure 5.1(a). Calculation of stress distributions using a finite element model (FEM) showed that different stress patterns could be produced in different parts of the sample by applying a stress along the neutral axis of the sample. For comparison with the FEM results, strain gauges were used to measure simultaneously the strains in the

sample plane along the directions perpendicular to, and at 45° on either side of, the neutral axis.

The magnetic imaging system used in this work consists of an x-y scanning frame and a signal processing module which were controlled using a personal computer [6]. During the measurements the sample was mounted on a vise and a compressive stress was applied along the neutral axis. The sample remained stationary while a sensor probe was scanned in steps of 1.27 mm over an area of 127 mm \times 102 mm to measure hysteresis loop and Barkhausen effect (BE) signals. The measurements were repeated under various applied compressive stresses up to -116 MPa. The measured signals were analyzed to extract the magnetic properties such as coercivity, remanence, permeability, hysteresis loss, from the hysteresis measurements; and rms value and total power from the BE signals. These measurement parameters were plotted as a function of the probe position using either a colour or grey scale to form two-dimensional images showing the spatial variations of the magnetic properties.

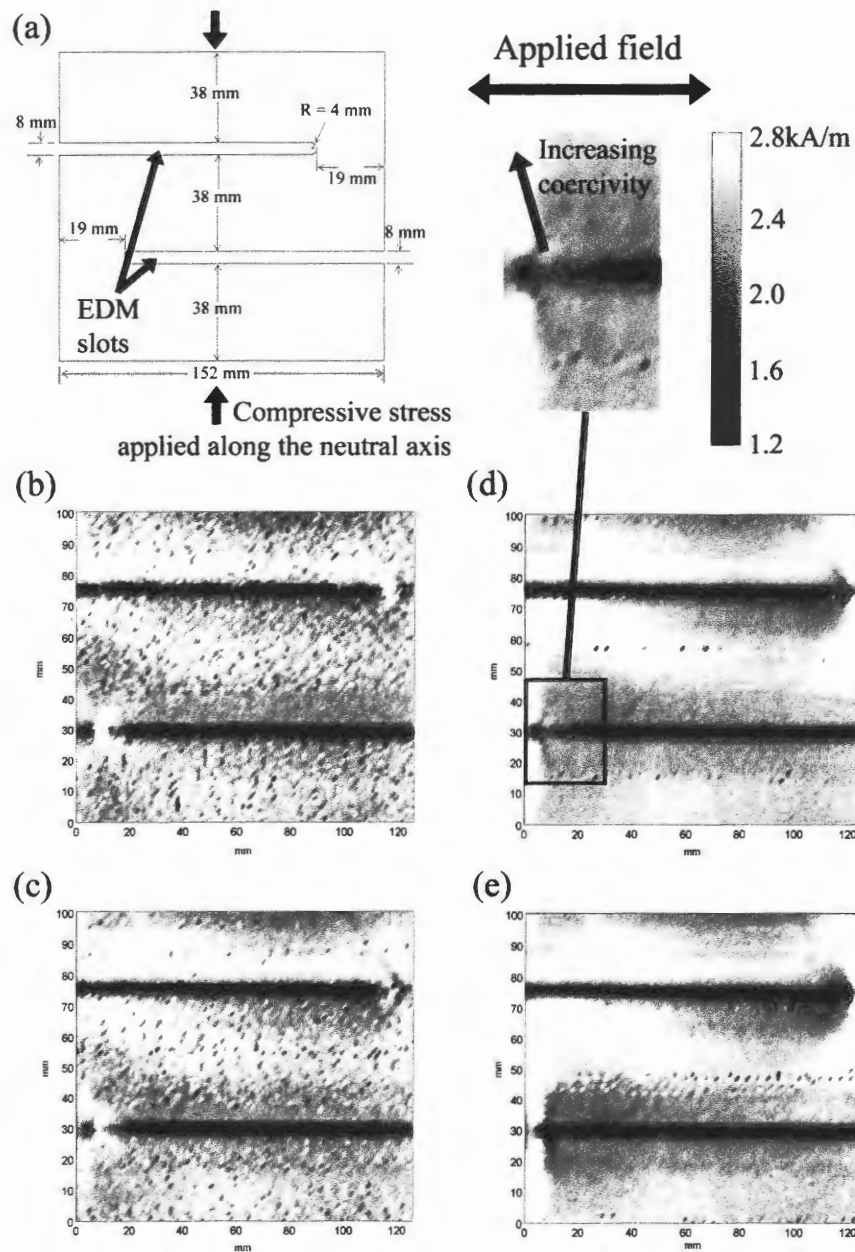


Figure 5.1. (a) The geometry and dimensions of the nickel plate. Scanned images of coercivity under compressive applied stresses of (b) 0 MPa, (c) -54 MPa, (d) -79 MPa and (e) -116 MPa. All images are of the same size (127 mm \times 102 mm) and use the same grey scale. Each of the images was constructed from the results of 8,000 individual hysteresis loop measurements. The inset is an enlarged image of (d) near the end of the bottom slot.

Results and Discussion

The scanned magnetic property images exhibit patterns indicative of non-uniform stress distributions in the sample. An example is given in Figure 5.1, which shows the measured coercivity images without any applied stress and under different compressive stresses applied along the neutral axis. Significant changes in image pattern were found near the ends of the slots as the applied stress was increased. In this region the coercivity exhibited a strong spatial variation. For example, under an applied stress of -79 MPa the coercivity increased from 1.87 kA/m (the coercivity at zero applied stress at this location is 1.97 kA/m) at the edge of the slot to 2.38 kA/m at 30 mm away from the slot (indicated by the arrow in the inset of Figure 5.1(d)). At the center of the sample a pattern emerged as the applied stress increased. In this region the change in coercivity with applied stress was less significant (the largest difference in coercivity is 0.25 kA/m under an applied stress of -79 MPa) than those measured near the ends of the slots.

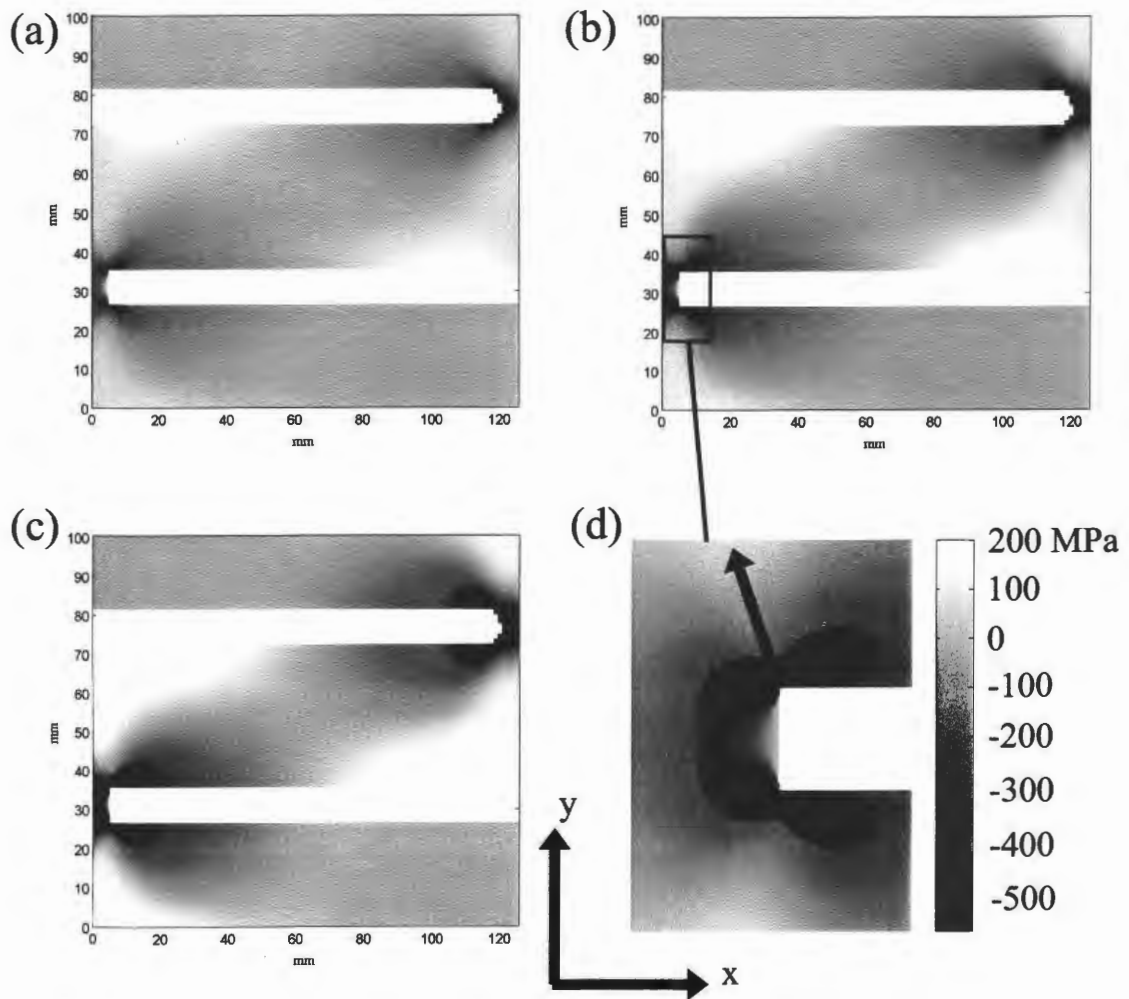


Figure 5.2. Stress component in the x-direction calculated using FEM for applied compressive stress of (a) -54 MPa, (b) -79 MPa and (c) -116 MPa. (d) An enlarged image showing that the stress component near the end of the slot changes from compressive to tensile.

To aid interpretation of the results, stress distributions in the sample were calculated using FEM. As shown in Figure 5.2, the calculated stress patterns are similar to the

measured coercivity images shown in Figure 5.1, particularly near the end of the slots. A high stress gradient is present in these regions where the stress component along the field direction changes from compressive at the edge of the slot to tensile in the surrounding region. The observed increase in coercivity with increasing distance from the end of the slot can be interpreted in the context of stress-induced anisotropy, in which for nickel with a negative magnetostriction coefficient, coercivity increases with tension but decreases with compression [7,8].

To evaluate the feasibility of detecting stress distribution by magnetic measurements, stress patterns were determined empirically from the measured spatial variations of magnetic properties. This was carried out by measuring *in situ* the magnetic properties of a nickel rod subjected to various uniaxial stresses within the elastic limit of the sample. The experimental calibration curve of the stress dependence of the normalized coercivity, as shown in Fig. 5.3, showed a sigmoidal shape which can be described empirically using the function

$$\frac{H_c(\sigma)}{H_c(0)} = \frac{A_1 - A_2}{1 + e^{(\sigma - \sigma_0)/c}} + A_2 \quad , \quad (\text{Equation 1})$$

where $H_c(0)$ is the coercivity under zero stress and $H_c(\sigma)$ is the coercivity at the applied stress σ . The function parameters A_1 , A_2 , σ_0 and c were determined empirically by curve fitting to be $A_1 = 0.355$, $A_2 = 1.270$, $\sigma_0 = -50.0$ MPa and $c = 61.3$ MPa.

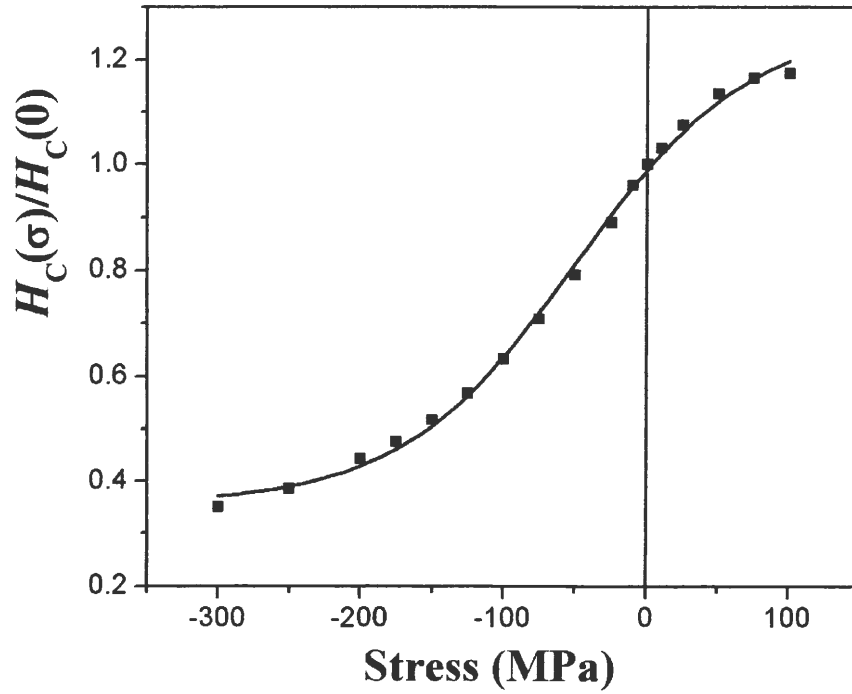


Figure 5.3. Measured stress dependence of coercivity $H_c(\sigma)$ normalized to the zero-stress value $H_c(0)$ for the nickel sample. The solid line is a fit to the experimental data using the function given in equation (1).

To estimate the stress component at each location of magnetic measurement, the ratio of the coercivity value measured under an applied stress to that measured under zero stress at that location was first calculated. The stress value was then estimated from the calibration curve shown in Figure 5.3. The result was plotted as a function of location in two dimensions using a color or grey scale to form images showing the stress distributions in the sample under different applied stresses.

As shown in Figure 5.4, the stress distributions determined from the measured coercivity values exhibited patterns near the ends of the slots that closely resembled those of

the FEM results (Figure 5.2). However a discrepancy was also observed, in particular along the side of the slot at the top and at the center of the sample (compare Figures 5.2(c) and 5.4(c)). It is noted that in these regions the difference between the stress values calculated by FEM and those determined empirically from measured coercivity values became larger as the applied stress was increased. A possible reason is that there may already have been residual plastic deformation in these regions that gave rise to non-uniform mechanical properties (e.g. elastic modulus) and therefore produced stress distributions different from the results of the FEM calculation which assumed that the mechanical properties were homogeneous throughout the material.

Conclusions

The feasibility of detecting surface stress distribution in a S-shaped nickel plate through magnetic measurements has been studied by measuring the spatial variations of magnetic properties using a magnetic imaging system. The image of measured coercivity exhibited features that resembled the stress patterns calculated using a finite element model. Stress distributions were determined empirically from measured coercivity values, and were found to exhibit patterns similar to those calculated using finite element model, particularly in regions where a high stress level or a high stress gradient exists. The results show that the magnetic imaging technique can be used for non-invasively detecting stress concentration in magnetic materials.

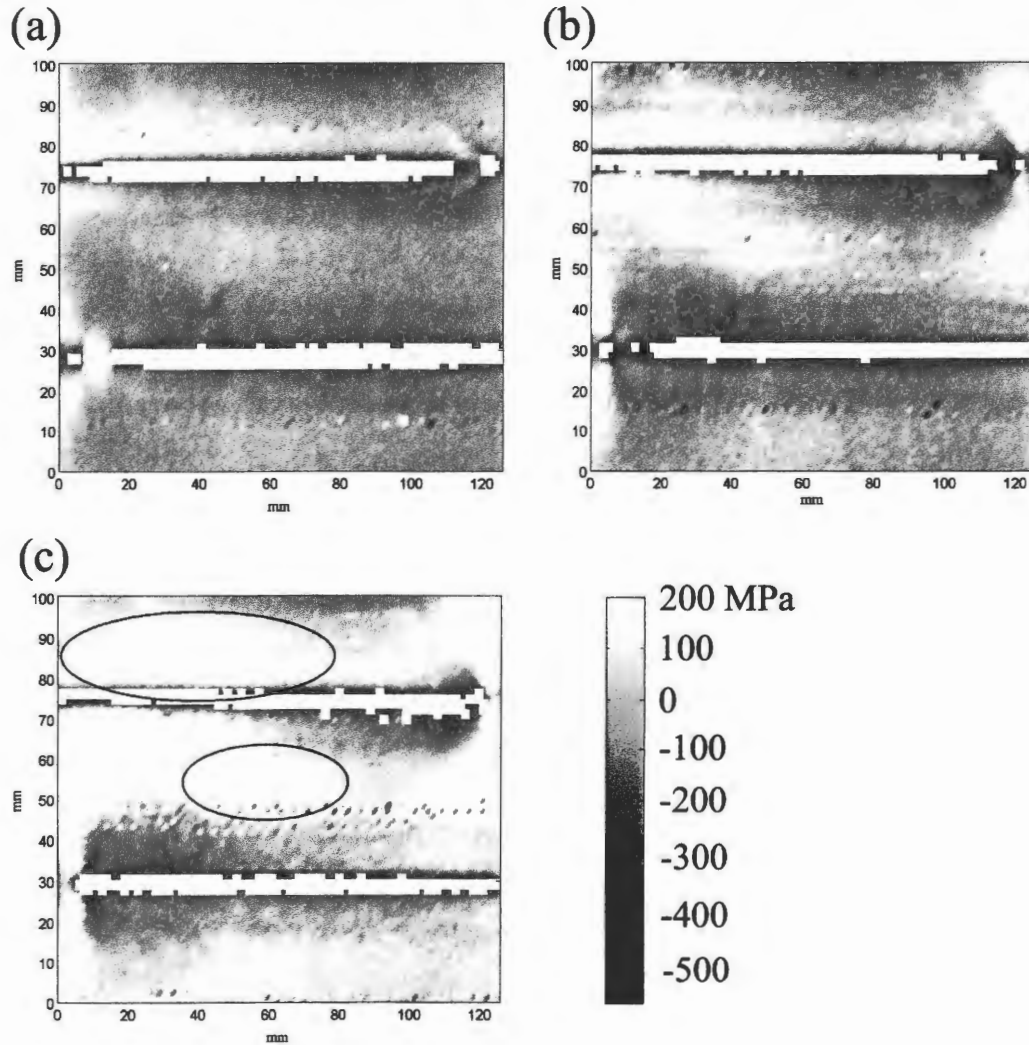


Figure 5-4. Stress component in the x-direction determined empirically from the measured coercivity values (Figure 5.1) for applied compressive stress of (a) -54 MPa, (b) -79 MPa and (c) -116 MPa. The circled regions in (c) exhibit tensile stress values higher than those calculated using FEM (Figure 5.2 (c)).

Acknowledgement

This work was supported by the NSF Industry/University Cooperative Research Program at the Center for Nondestructive Evaluation, Iowa State University.

References

1. D.C. Jiles, "Theory of the magnetomechanical effect", *J. Phys. D: Applied Physics*, 28, 1537, 1995.
2. D.C. Jiles, "Magnetic methods in nondestructive testing", *Encyclopedia of Materials Science and Technology*, p. 6021. Ed. K.H.J. Buschow *et al.*, Elsevier Press, Oxford, September 2001.
3. M.J. Sablik, "Hysteresis Modeling of the Effects of Stress on Magnetic Properties and Its Application to Barkhausen NDE." *Current Topics in Magnetism Research*. Trivandrum, India: Office of Scientific Information, Research Trends (1994).
4. J. Gauthier, T.W. Krause and D.L. Atherton, "Measurement of residual stress in steel using the magnetic Barkhausen noise technique", *NDT&E International*, Vol. 31, No. 1, pp. 23-31, 1998.
5. S. Tiitto, in 'Handbook of measurement of residual stresses', Part 8: Magnetic Methods (ed. J. Lu), pp. 179 – 224; 1996, Lilburn, GA, Society for Experimental Mechanics.

6. C.C.H. Lo, J.A. Paulsen and D.C. Jiles, "Development of a magnetic NDE imaging system using magnetoresistive devices". Proceedings of the 29th *Annual Review of Progress in Quantitative NDE*, Vol. 22A, pp. 931-938, 2003.
7. D.C. Jiles, T.T. Chang, D.R. Hougen and R. Ranjan, "Stress-induced changes in the magnetic properties of some nickel-copper and nickel-cobalt alloys", *J. Appl. Phys.*, 64(7), 3620, 1988.
8. C.C.H. Lo, S.J. Lee, L. Li, L.C. Kerdus and D.C. Jiles, "Modeling of stress effects on magnetic hysteresis and Barkhausen emission using an integrated hysteretic-stochastic model", *IEEE Trans. Magn.*, 38, pp.2418-2420, 2002.

CHAPTER 6. CONCLUSIONS

Two new magnetic methods for the detection of stress levels in a material have been investigated. One is based on the measurement of the magnetic properties of the material under test; the other is based on the development of a new magnetoelastic material that shows high sensitivity of magnetization to stress. The conclusions drawn from the progress with these methods are given in this chapter.

Magnetostrictive stress sensing material

Magnetostrictive materials have been identified as likely candidates for use in a new generation of stress and torque sensors. Cobalt ferrite has specifically been singled out for this purpose because it is low in cost, corrosion resistant and has good mechanical properties. Despite this, the presence of a magnetomechanical hysteresis at room temperature of 0.7 N.m in toroid shaped torque sensor samples has been identified as a major problem with the stress sensing capabilities of the material because a linear behavior is preferred and if not then non-linear but hysteresis free behavior is acceptable.

These studies have shown that progress has been made in the development of a new material for use in a magnetomechanical stress sensor. This progress has led to the development and characterization of two new ranges of material compositions consisting of silicon and manganese-substituted cobalt ferrite materials ($\text{Co}_{1+x}\text{Si}_x\text{Fe}_{2-2x}\text{O}_4$ and $\text{Co}_1\text{Fe}_{2-x}\text{Mn}_x\text{O}_4$) that improves upon the previously studied pure cobalt ferrite material. The newly discovered silicon-substituted cobalt ferrite was shown to be an improvement to pure cobalt

ferrite by lowering the Curie temperature by as much as 44°C however the material was difficult to produce. This was because some silicon was causing the formation of a second phase SiO_2 in the material and even more silicon was being lost somewhere in the process. Since the processing conditions had a very large effect on the end product, the magnetic properties of the material were difficult to characterize. For these reasons, manganese-substituted cobalt ferrite was examined.

A manganese substituted cobalt ferrite family of materials was also produced and characterized. It was found to be a much more likely candidate for stress sensing applications because the Curie temperature could be reduced by as much as 390°C and in turn should reduce the magnetomechanical hysteresis present at room temperature and below, without an unacceptable loss of sensitivity. Continuation of this study will likely be with a manganese substituted cobalt ferrite material ($\text{Co}_1\text{Fe}_{2-x}\text{Mn}_x\text{O}_4$) with manganese content of between $x=0.2$ and $x=0.3$. This will give a suitable decrease of the Curie temperature of about 90°C with only a moderate decrease of maximum magnetostriction of about 80 ppm. This discovery has also made it possible to “tune” the stress sensing capabilities of the material for a variety of applications by slightly adjusting the composition of the material. This study found that the processing parameters did affect the material, however the final product was much more controllable than the silicon-substituted material. Further work needs to be performed to examine the feasibility of using the newly developed material as an actual working magnetic stress sensor.

Magnetic imaging system

The design, development, and testing of a new magnetic imaging system was also a major component of this thesis. It was found that this system could be used to create images of the spatial variation of the magnetic properties of a material to help locate variations of the material condition. A description of how the system works was given along with some images obtained from the system. The software package that was developed for controlling the scanning process, acquiring and analyzing the detected magnetic signals, and converting the measured magnetic properties into images was proven to work well for the applications used in these studies. The system was shown to have a minimum step size of 0.025 mm with a maximum scan size of 250 mm by 250 mm.

It has been proven that the system is capable of detecting surface cracks as small as 0.25 mm wide and sub-surface notches that are 6 mm below the material surface in steel plates. When detecting surface notches, it was found that the hysteresis measurements produced better results than the Barkhausen scans because the Barkhausen measurements can only obtain information about a very thin surface layer of the material. This study also showed that the depth of a crack affects the color contrast in the images more than the width. Thickness variations as deep as 7.5 mm in steel plates were also detectable with the system using the hysteresis measurement function.

It has also been shown that the magnetic imaging system is capable of detecting stress levels in nickel. This was done by compressing a nickel plate that was cut into a shear beam load cell configuration and scanning it with the imaging system. The plate was

scanned with no external forces being applied, and with a stress of -54 MPa, -79 MPa, and -116 MPa. The resulting magnetic images showed stress distributions similar in shape to the stress distributions produced by finite element modeling. The results from the scans with the plate under stress were then normalized with the un-stressed scans and a calibration curve was used to calculate the stress distribution. These calculated stress distribution images showed close resemblance to those produced with finite element modeling. This indicates that the magnetic imaging system is capable of determining stress variations and may be an accurate method for measuring both applied and residual stress distributions.

More work on this system needs to be performed before it will be an attractive solution for non-destructive detection of stress. This future work needs to include new probe designs to increase the spatial resolution of the scan and to account for non-planer surfaces. The scan speed also needs to be increased, possibly by a more optimized software package or new probes with sensor arrays. More work with finite element modeling also needs to be performed to make the results more quantitative than qualitative.

Magnetic Stress Detection

The use of magnetic measurement methods in the detection of stress levels present in a material can be a very powerful technique and has great potential in a variety of applications, however, future research and development needs to be performed before either of these methods will be attractive to the industrial market.